PERFORMANCE CHARTS FOR THE TURBOJET ENGINE

By Benjamin Pinkel and Irving M. Karp

National Advisory Committee for Aeronautics
Aircraft Engine Research Laboratory
Cleveland Airport, Cleveland, Ohio.

SUMMARY

Charts are presented for computing the thrust, fuel consumption, and other performance values of a turbojet engine for any given set of operating conditions and component efficiencies. The effects of the pressure losses in the inlet duct and combustion chamber, the variation in the physical properties of the gas as it passes through the cycle, and the change in mass flow by the addition of fuel are included. The principal performance charts show the effects of the primary variables and correction charts provide the effects of the secondary variables.

Some of the performance and operational characteristics [illegible] turbojet engine are illustrated by a discussion of [illegible] typical cases. It is shown for example that although [illegible] per unit mass rate of air flow increases with increased [illegible] tor discharge temperature, for minimum specific fuel [illegible] ption, an optimum combustor outlet temperature exists [illegible] some cases may be less than the limiting temperature [illegible] strength-temperature characteristics of present [illegible] The influence of the characteristics of a given [illegible] and turbine on the performance of a turbojet engine [illegible] these given components is discussed for the cases [illegible] with a centrifugal compressor and for an engine with [illegible] compressor.

INTRODUCTION

[illegible] ynamic studies have been made of turbojet [illegible] quations or charts for obtaining the engine [illegible] esented and in which performance trends are [illegible] es 1, 2, 3, and 4). A study of design and [illegible] elating to turbojet engines is given in [illegible] The purpose of the present paper to [illegible] h a factor indicative of the engine [illegible] n terms of the important design and

operating parameters. By this means the engine performance for a given set of parameters can be quickly evaluated and an insight is provided into the degree of change of performance possible through change in the design parameters. The principal performance chart contains only the important parameters. The effect of minor parameters are introduced through a correction factor given in a supplementary chart.

In order to show some of the more important characteristics of the turbojet engine several illustrative cases are discussed. The effects of compressor pressure ratio and combustor outlet temperature on the thrust and specific fuel consumption are illustrated as well as the decrease in compressor efficiency with increasing pressure ratio. The performance characteristics of typical components of the turbojet engine, that is, a turbine, a centrifugal compressor, and an axial flow compressor are given. The influence of the characteristics of these components on the performance of the turbojet engine constructed therefrom is illustrated for an engine containing a centrifugal compressor, and for an engine containing an axial flow compressor.

ANALYSIS

A diagram of the jet-propulsion device under discussion is shown in figure 1. Air is inducted into the intake of the engine and delivered to the compressor inlet. Part of the dynamic pressure of the free air stream is converted into static pressure at the compressor inlet by the diffusing action of the inlet duct. The air is further compressed in passing through the compressor and is delivered to the combustion chamber where fuel is injected and burned. The products of combustion then pass through the turbine nozzles and buckets where an appreciable drop in pressure occurs and finally are discharged rearwardly through the discharge nozzle to provide thrust.

The variables affecting the performance are divided into a primary group and a secondary group. The variables of the primary group are shown on the principal charts for determining the performance of the jet-propulsion unit. The variables of the secondary group are shown on an auxiliary chart for determining a factor ϵ usually close to unity, which also appears as a variable on the principal performance charts.

The primary group of variables includes:

(a) Compressor efficiency η_c

(b) Compressor total-pressure ratio p_2/p_1

(c) Burner efficiency η_f

(d) Ratio of combustion-chamber outlet total temperature to free atmospheric temperature T_4/T_o

(e) Turbine efficiency η_t

(f) Airplane velocity V_o

(g) Atmospheric temperature T_o

(h) Discharge-nozzle velocity coefficient C_v, which includes losses in the tail pipe following the turbine

The second group includes:

(a) Drop in total pressure across the inlet ducting caused by friction and turbulence Δp_d

(b) Drop in total pressure across the combustion chamber caused by both the mechanical obstruction of the burners and the momentum increase of the gases during combustion $\Delta p_{(2-4)}$

(c) Effect of the difference between the physical properties of hot exhaust gases during the expansion processes and cold air (The effect of change in specific heat of the gas during the other processes is included in the principal charts.)

A chart is given from which a factor ϵ can be obtained corresponding to the values of the secondary group of variables. This factor ϵ appears in the parameters on the principal performance charts.

The significance of the symbols appearing in the charts and in the subsequent discussion are as follows:

A ratio of compressor pressure ratio p_2/p_1 to reference pressure ratio $(p_2/p_1)_{ref}$

A_n effective exhaust nozzle area, sq. ft.

a, b, c	factors that measure effects produced by secondary variables
B	ratio of tip speed of compressor to blade speed (pitch line) of turbine
C_v	velocity coefficient of discharge nozzle
F	net thrust, (lb)
f	fuel-air ratio
h	lower heating value of fuel, (Btu/lb)
J	mechanical equivalent of heat, 778 (ft-lb/Btu)
K_a	ratio of the compressor power per unit mass rate of air flow to the square of the compressor tip speed, P_c/MU^2
M	mass rate of air flow, (slug/sec)
P_o	atmospheric free-air static pressure, (lb/sq ft absolute)
P_1	total pressure at compressor inlet, (lb/sq ft absolute)
P_2	total pressure at compressor outlet, (lb/sq ft absolute)
P_4	total pressure at turbine inlet, (lb/sq ft absolute)
Δp_d	drop in total pressure across inlet duct, (lb/sq ft)
$\Delta p_{(2-4)}$	over-all drop in total pressure across combustion chamber due to mechanical obstruction of the burners and momentum increase of gases during combustion, (lb/sq ft)
P_{5s}	static pressure at turbine outlet
P_c	compressor-shaft horsepower input
r	$\Delta p_{(2-4)}/P_2$
T_o	atmospheric temperature, (^oR)

T_1 compressor-inlet total temperature, (°R)

T_2 compressor-outlet total temperature, (°R)

T_4 combustion-chamber outlet total temperature, (°R)

V_o airplane velocity, (ft/sec)

V_5 axial component of gas velocity at turbine discharge, (ft/sec)

V_j jet velocity, (ft/sec)

ΔV_j increase in jet velocity due to effect of turbine-loss reheat, (ft/sec)

V_t theoretical turbine nozzle jet velocity corresponding to ideal expansion of gas from turbine inlet total pressure and temperature to turbine outlet static pressure, (ft/sec)

u turbine blade speed measured at turbine pitch line, (ft/sec)

U compressor tip speed, (ft/sec)

W_f weight flow of fuel, (lb/hr)

Y ratio of ram temperature rise to free-air atmospheric temperature, $V_o^2/2\,J\,c_{pa}\,T_o$

Z ratio of compressor power per unit mass rate of air flow to enthalpy of air at temperature T_o, $550\,P_c/J\,c_{pa}\,M\,T_o$

γ_a ratio of specific heats of air

ϵ correction factor that accounts for over-all effects produced by secondary variables

η_c compressor efficiency, i.e. ideal work in compressing air adiabatically from compressor inlet total temperature and pressure to compressor outlet total pressure divided by the compressor shaft power

η_c' compressor stage efficiency

η_f efficiency of combustion of fuel in combustion chamber

η_t turbine efficiency, i.e. turbine shaft power divided by the ideal power of the gas jet expanding adiabatically from turbine inlet total pressure and temperature to the turbine outlet static pressure less the kinetic power corresponding to the average axial velocity of the gas at the turbine exit,

$$\eta_t = \frac{\text{Turbine shaft power}}{\frac{1}{2}\dot{M}_t V_t^2 - \frac{1}{2}\dot{M}_t V_5^2}$$

η'_t turbine efficiency, i.e. turbine shaft power divided by the ideal power of the gas jet expanding adiabatically from turbine inlet total pressure and temperature to turbine outlet static pressure,

$$\eta'_t = \frac{\text{Turbine shaft power}}{\frac{1}{2}\dot{M}_t V_t^2}$$

δ ratio of pressure to standard sea level pressure (2116 lbs/sq ft), i.e. $\delta_o = p_o/2116$, $\delta_1 = p_1/2116$, etc.

θ ratio of temperature to standard sea level temperature (519°R), i.e. $\theta_o = T_o/519$, $\theta_1 = T_1/519$, etc.

$$(p_2/p_1)_{ref} = \left[\left(\frac{1}{1+Y}\right)^2 \eta_c \eta_t \epsilon \frac{T_4}{T_o}\right]^{\frac{\gamma_a}{2(\gamma_a - 1)}}$$

The equations from which the charts are prepared are listed in appendix A and are derived in reference 6.

DISCUSSION OF CHARTS

Useful equations. - The net thrust of the jet-propulsion device, when the effect of the fuel weight is neglected, is given by the equation

$$F = \dot{M}(V_j - V_o) \qquad (1a)$$

When the effect of fuel weight is included, the thrust is given by

$$F = \dot{M} (V_j - V_o) + f \dot{M} V_j \qquad (1b)$$

The net thrust horsepower thp is given by

$$thp = F V_o/550 \qquad (2)$$

The compressor-shaft horsepower per slug per second of air is expressed as

$$P_c/\dot{M} = J c_{pa} T_o Z/550 = 5675 Z (T_o/519) \qquad (3)$$

The compressor-inlet total temperature is obtained from

$$T_1/T_o = 1 + Y \qquad (4)$$

The fuel consumption per unit mass rate of air flow is given in terms of the fuel-air ratio by the following relation

$$W_f/\dot{M} = 115,920 f \qquad (5)$$

By means of equations (1) to (5) and the curves of figures 2 to 7 the performance of the turbojet engine and some associated quantities of interest can be readily determined. The curves are given in a form which shows the effects of the important variables and enables either very accurate computations or rapid but less accurate computations to be made.

Curves for obtaining the flight Mach number, the values of Y, and the compressor-inlet total pressure for various values of the factor $V_o \sqrt{519/T_o}$ are shown in figure 2. The compressor-inlet total temperature is obtained from the value of Y and equation (4).

The quantity $\eta_c Z$ is plotted against the compressor total-pressure ratio and Y in figure 3. The compressor power (and hence the turbine power) is computed from equation (3) and the value of Z. The effect of the variation in the specific heat of air c_{pa} during compression is neglected in this plot, the error introduced being less than 1 percent for the range of compressor pressure ratios shown in figure 3 and for compressor inlet temperatures up to 550° R.

The value of $(p_2/p_1)_{ref}$ plotted against the factor $\eta_c \eta_t \epsilon \frac{T_4}{T_o} \left(\frac{1}{1+Y}\right)^2$ is also given in figure 3. The actual compressor pressure ratio p_2/p_1 divided by the quantity $(p_2/p_1)_{ref}$ defines the value of the factor A used in figure 4(a). The factor ϵ accounts for the effects of pressure losses in the inlet duct to the system, pressure drop in the combustion chamber, and the deviation from the value of the specific heat of air at 519° R of the specific heats of the gases during the expansion through the turbine and the nozzle. In a well designed system the value of ϵ is close to or slightly greater than unity.

From the left-hand set of curves of figure 4(a), the jet-velocity factor $V_j\sqrt{\frac{\eta_c\eta_t}{C_v^2}}\sqrt{\frac{519}{T_o}}$ can be determined as a function of $\eta_c\eta_t \epsilon \frac{T_4}{T_o}$ and the parameter A or 1/A for zero flight speed. (When A is less than unity, the value of 1/A is used in reading values from fig. 4(a).) The jet-velocity factor can be obtained for airplane velocities other than zero by moving horizontally across the graph to the desired velocity curve on the right-hand set of curves and then reading the value on the lower abscissa. The thrust can then be computed from the value of V_j and equation (1a). As previously mentioned, the value of A is found by dividing the compressor pressure ratio p_2/p_1 by the value of $(p_2/p_1)_{ref}$ obtained from figure 3 corresponding to the values of the parameters η_c, η_t, ϵ, T_4, T_o, and Y being investigated.

It is noted in figure 4(a) that for given values of η_c, η_t, T_4, and T_o, if ϵ remains constant as p_2/p_1 or A varies, then the variation of jet velocity with pressure ratio occurs along the constant $\eta_c\eta_t\epsilon\frac{T_4}{T_o}$ line. In this case, V_j has a maximum value when A is equal to unity, which occurs at a pressure ratio equal to $(p_2/p_1)_{ref}$. Actually, however, for a given unit as p_2/p_1 varies, the value of ϵ changes slightly and hence $\eta_c\eta_t\epsilon\frac{T_4}{T_o}$ changes, with the result that

V_j has a maximum value for a value of p_2/p_1 somewhat greater than $(p_2/p_1)_{ref}$. It should also be noted that $(p_2/p_1)_{ref}$ is changed by the change in ϵ and this new value must be used in computing the new value of A when p_2/p_1 is varied. In any event, the value of V_j corresponding to A = 1 is a close approximation to the jet velocity for maximum thrust per unit mass rate of air flow M for a given set of values of T_4, T_o, and component efficiencies. Similarly for a case in which η_c varies with p_2/p_1 consideration of figures 3 and 4(a) show that the maximum value of V_j occurs at a value of A somewhat different from unity.

As an example of the use of figures 2, 3, and 4(a) for a rapid approximate computation of the thrust per unit mass rate of air flow, F/M, consider the following case:

Discharge nozzle velocity coefficient, C_v	0.90
Compressor efficiency, η_c	0.85
Turbine efficiency, η_t	0.90
Turbine inlet temperature, T_4 °R	2000
Atmospheric temperature, T_o °R	500
Airplane velocity, V_o, ft/sec	733
Compressor pressure ratio, p_2/p_1	4
Assume ϵ = 1, then from the above quantities	
$V_o\sqrt{519/T_o}$, ft/sec	747
Y (from figure 2)	0.089
$\eta_c\eta_t \epsilon T_4/T_o$	3.06
$\eta_c\eta_t \epsilon T_4/T_o(1+Y)^2$	2.58
$(p_2/p_1)_{ref}$ (from figure 3)	5.25
1/A	1.31
$V_j\sqrt{\frac{\eta_c\eta_t}{C_v^2}}\sqrt{\frac{519}{T_o}}$ (from figure 4(a)), ft/sec	2000
V_j, ft/sec	2020

F/M (equation 1(a)), lb/(slug/sec) 1287

Subsequent charts and discussion introduce corrections that permit a high degree of accuracy when desired.

The losses in kinetic energy in the turbine passages appear as heat energy in the gas leaving the turbine. This energy will be termed "turbine-loss reheat." If there is further expansion of the gas in passing through the jet nozzle (caused by a reduction in static pressure in passing from the turbine exit to the jet-nozzle exit), a conversion of part of the turbine-loss reheat to kinetic energy occurs in the jet. If, however, the velocity at the turbine exit is substantially equal to the final jet velocity, no further expansion occurs and no kinetic energy is recovered from the turbine-loss reheat. The curves of figure 4(a) correspond to this case. The ratio of the increase in jet velocity to the final jet velocity $\Delta V_j/V_j$ obtained when the velocity at the turbine discharge V_5 is less than the final jet velocity is shown in figure 4(b).

Figure 4(b) shows that $\Delta V_j/V_j = 0$ when $C_v V_5/V_j = 1$ for all values of turbine efficiency. It is also noted that $\Delta V_j/V_j$ approaches 0 as turbine efficiency approaches 1 for all values of $C_v V_5/V_j$ because the turbine-loss reheat approaches 0 with increase in turbine efficiency.

It is evident from figure 4(b) that, for a given turbine efficiency, the smaller the ratio of $C_v V_5/V_j$, the greater is the recovery of turbine-loss reheat. Decrease in turbine-discharge velocity V_5 is obtained by increase in annular area swept by the turbine buckets. Bucket stress is one of the principal limitations on bucket height and thus on bucket-annulus area.

The compressor-outlet total temperature T_2 plotted against the factor $T_0 (1 + Y + Z)$ is shown in figure 5. This curve includes the variation in the specific heat of the air during compression and was computed using reference 7.

The fuel-air ratio factor η_f is plotted in figure 6 against $T_4 - T_2$ (the rise in total temperature in the combustion chamber) for various values of T_4. These curves were constructed using reference 8 based on the latest avail-

able information on specific heats of air and exhaust-gas mixtures and are for a fuel having a lower heating value of 18,900 Btu per pound and a hydrogen-carbon ratio of 0.185. For fuels having other values of h, the value of f given in figure 6 is corrected accurately by multiplying it by the factor $18{,}900/h$. The effect of the hydrogen-carbon ratio of the fuel on f is generally small and for a range of hydrogen-carbon ratios from 0.16 to 0.21 the error due to the deviation from the value of 0.185 is less than one-half of 1 percent. The fuel consumption per unit mass rate of air flow is obtained from the value of f and equation (5).

The value of ϵ, which takes care of the effect of the secondary group of variables, is obtained from figure 7. The quantity ϵ is given by the relation $\epsilon = 1 - a - b + c$, where a, b, and c are given in figure 7. The effect of the drop in total pressure across the inlet duct Δp_d is shown in figure 7(a). The effect of the over-all drop in total pressure across the combustion chamber $\Delta p_{(2-4)}$ is introduced in figure 7(b). Reference 9, which discusses combustion in a chamber of constant flow area, is useful in evaluating the momentum-pressure drop in the combustion chamber. A correction for the difference between the physical properties of the hot gases and the cold air, involved in the computation of the expansion processes through the turbine and the jet nozzle is given in figure 7(c). Although ϵ does not differ appreciably from unity, a change in ϵ of 1 percent in some cases may introduce a change of several percent in the thrust.

In the discussion of the charts, the effect of the weight of injected fuel was not mentioned. It is shown in appendix C of reference 6 that the effect of the weight of fuel on the jet velocity can be taken into account by using for the value of η_t in the charts the product of the turbine efficiency and $(1 + f)$. This term appears in the factor $\eta_c \eta_t \epsilon \frac{T_4}{T_o} \left(\frac{1}{1 + f} \right)^2$ in figure 3 used in finding $(p_2/p_1)_{ref}$ and in the factors $\eta_c \eta_t \epsilon \frac{T_4}{T_o}$ and $V_j \sqrt{\eta_c \eta_t / C_v^2} \sqrt{519/T_o}$ of figure 4(a). The value of V_j determined is then used in equation (1b) which takes into account the additional weight of fuel introduced.

As an example of the use of these figures, consider a system having the following performance and operating parameters:

1. Compressor efficiency η_c	0.80
2. Turbine efficiency η_t	0.90
3. Combustion efficiency η_f	0.97
4. Discharge-nozzle velocity coefficient C_v	0.96
5. Airplane velocity V_o, (ft/sec)	733
6. Compressor total-pressure ratio p_2/p_1	6
7. Atmospheric free-air static pressure p_o, (in. Hg)	29.9
8. Atmospheric temperature T_o, ($^\circ$R)	519
9. Combustion-chamber outlet total temperature T_4, ($^\circ$R)	1960
10. Drop in total pressure across inlet duct Δp_d, (in. Hg)	0.5
11. Drop in total pressure across combustion chamber $\Delta p_{(2-4)}$, (in. Hg)	3
12. h, (Btu/lb)	18,800

(a) Determination of Y and flight Mach number

From items 5 and 8

13. $V_o\sqrt{\frac{519}{T_o}}$, (ft/sec)	733

From item 13 and figure 2

14. Y	0.0861
15. Flight Mach number	0.656

(b) Determination of Z and compressor power

Using items 6 and 14, read on figure 3

16. $\eta_c Z$	0.726

From items 16 and 1

17. Z	0.908

Using items 17 and 8 in equation (3) the compressor power per unit mass rate of air flow is

18. P_c/M, (hp)/(slug/sec)	5153

(c) Determination of fuel-air ratio and fuel consumption

From items 8, 14, and 17

19. $T_o(1 + Y + Z)$, ($^\circ$R)	1035

Using item 19 and figure 5

20. T_2, (°R) 1025

From items 20 and 9

21. $T_4 - T_2$, (°F) 935

From items 21 and 9 and figure 6

22. $\eta_f f$ 0.01372

Using items 22 and 3

23. f 0.01414

Since the lower heating value of the fuel is equal to 18,500 Btu per pound (item 12), item 23 has to be multiplied by the factor $\frac{18,900}{18,500}$ and the adjusted value is

24. f 0.01445

From item 24 and equation (5)

25. W_f/M, (lb/hr)/(slug/sec) 1675

(d) Determination of the factor ϵ

From items 7, 10, and 11

26. $\Delta p_d/P_o$ 0.017
27. $\Delta p_{(2-4)}/P_o$ 0.10

while from items 14 and 16

28. $Y + \eta_c Z$ 0.812

Using items 26, 28, and figure 7(a)

29. a 0.006

Using items 27, 28, and figure 7(b)

30. b 0.004

From figure 2 and item 13

31. $\frac{p_1 + \Delta p_d}{p_o}$ 1.335

From items 31, 26, and 6

32. $\frac{p_2}{p_o}$ 7.91

which when used with item 9 in figure 7(c) gives

33. e 0.035

From items 29, 30, and 33

34. $\epsilon = 1 - .006 - .004 + .035$ 1.025

(c) Determination of $(p_2/p_1)_{ref}$ and A

Using items 1, 2, 34, 9, 8, and 14

35. $\eta_c \eta_t \epsilon \frac{T_4}{T_o} \left(\frac{1}{1 + Y}\right)^2$ 2.363

From item 35 and figure 3

36. $(p_2/p_1)_{ref}$ 4.50

From items 6 and 36

37. A 1.333

(f) Determination of jet velocity, net thrust per unit mass rate of air flow, and other performance quantities

Using items 1, 2, 34, 9, and 8

38. $\eta_c \eta_t \epsilon \frac{T_4}{T_o}$ 2.787

From items 38, 37, 13, and figure 4(a) the jet-velocity factor is

39. $V_j \sqrt{\frac{\eta_c \eta_t}{C_v^2}} \sqrt{\frac{519}{T_o}}$, (ft/sec) 1806

and from items 39, 1, 2, 4, and 8

40. V_j, (ft/sec) 2044

The net thrust per unit mass rate of air flow is obtained from items 40, 8, and equation (1a)

41. F/M, (lb)/(slug/sec) 1311

The thrust horsepower per unit mass rate of air flow is calculated from items 41, 8, and equation (2)

42. thp/M, (thp)/(slug/sec) 1747

From items 25 and 41

43. W_f/F, (lb/hr)/(lb thrust) 1.278

and from items 25 and 42

44. W_f/thp, (lb)/(thp-hr) 0.959

(g) Effect of the weight of injected fuel and turbine-loss reheat on jet velocity and thrust

Where more accurate results are desired, the calculations are made taking into account the effect of the weight of fuel introduced and the effect of turbine-loss reheat. The effect of the fuel on jet velocity is handled by using for the value of η_t the product of the turbine efficiency and $(1 + f)$. This will now be done for the case just considered.

From items 24 and 35

45. $\eta_c \eta_t \epsilon \frac{T_4}{T_0} \left(\frac{1}{1+Y}\right)^2$ 2.396

From figure 3 the corresponding

46. $(p_g/p_1)_{ref}$ 4.61

From items 6 and 46

47. A 1.30

Similarly accounting for fuel flow, item 38 becomes

48. $\eta_c \eta_t \epsilon \frac{T_4}{T_0}$ 2.827

so that from items, 47, 48, and 13, and figure 4(a)

49. $V_j \sqrt{\frac{\eta_c \eta_t}{C_v^2}} \sqrt{\frac{519}{T_o}}$, (ft/sec) 1838

Again taking into account the effect of fuel by adjusting the η_t term

50. V_j, (ft/sec) 2065

which differs from item 40 by 1 percent

The effect of reheat may be important when η_t is considerably less than unity and the velocity at turbine discharge is appreciably less than the final jet velocity. Let it be assumed in the example being discussed that the turbine is designed to have a discharge velocity of

51. V_5, (ft/sec) 700

Then from items 4, 50, and 51

52. $C_v V_5/V_j$ 0.33

From items 8, 9, and 17

53. $\frac{T_4}{T_o Z}$ 4.16

From figure 4(b) corresponding to items 2, 52, and 53

54. $\Delta V_j/V_j$ 0.012

and from items 50 and 54

55. ΔV_j, (ft/sec) 25

Using items 55 and 50

56. Corrected V_j, (ft/sec) 2090

Thus in this case, reheat provides an additional 1 percent increase in the value of V_j.

The thrust per unit mass rate of air flow is obtained from items 56, 5, and equation (1b)

57. F/M, (lb)/(slug/sec) 1357

compared with 1311 where the effects of fuel and reheat were neglected.

From equation (2) and items 37 and 5

58. thp/M, (thp)/(slug/sec) 1808

and using items 25 and 57

59. W_f/F, (lb/hr)/(lb) 1.234

and items 25 and 58 give

60. W_f/thp, (lb/thp-hr) 0.926

JET-PROPULSION-UNIT PERFORMANCE

For the illustration of the performance and some of the characteristics of the subject jet-propulsion system, several cases of interest will be discussed.

The following parameters are assumed:

Compressor efficiency η_c	0.85
Turbine efficiency η_t	0.90
Discharge-nozzle velocity coefficient C_v	0.97
Combustion efficiency η_f	0.96
Heating value of fuel h, (Btu/lb)	18,900
ϵ	1.00

These compressor and turbine efficiencies are not unreasonably high when it is considered that in the definition of efficiency in this report the compressor and the turbine are credited with the kinetic energy of the gases at the compressor and turbine exits, respectively.

The computed turbojet performance in this illustrative case includes the contribution of the fuel weight.

The values of component efficiencies and ϵ for any given turbojet engine vary with altitude and flight speed. In the present computations, the component efficiencies and ϵ were assumed constant at the values listed, hence, the illustrative

curves represent the performance of a series of turbojet engines having the listed characteristics. One curve is also given for a case in which the variation of ϵ with compressor pressure ratio is considered.

When $V_o = 0$, $T_o = 519^\circ$ R, figure 8 shows the rate of fuel consumption per unit thrust and the static thrust per unit mass rate of air flow plotted against the compressor pressure ratio for various values of the gas total temperature at the combustion-chamber exit. It is noted that minimum specific fuel consumption occurs at a higher compressor pressure ratio than maximum thrust per unit mass rate of airflow. A curve for $T_4 = 1960^\circ$R where the variation in ϵ with p_2/p_1 is considered is also shown in figure 8. For this curve, values of $\Delta p_d/p_o = 0.04$ and $\Delta p_{(2-4)}/p_o = 0.10$ were chosen and assumed to remain constant. (For a given unit, however, $\Delta p_{(2-4)}$ will also vary with p_2/p_1 so that the determination of the actual variation in ϵ with compressor pressure ratio becomes quite complex.) It is seen from figure 8 that the value of compressor pressure ratio for a maximum value of F/M is greater for the case where ϵ varies with pressure ratio than for the case where ϵ is assumed constant, and that the peak value of F/M for the first case is slightly higher than that for the second case.

Figure 9(a) is a replot of figure 8 and shows compressor pressure ratio and fuel consumption per unit thrust plotted against thrust per unit mass rate of air flow. Similar curves are presented in figures 9(b) and 9(c) for other combinations of atmospheric temperature and airplane velocity. A scale of specific fuel consumption in pounds per thrust horsepower-hour is added on figures 9(b) and 9(c).

The amount of air handled by a unit is limited by the diameter of the unit. When high thrust per unit mass rate of air flow rather than low specific fuel consumption is the primary consideration, it is apparent from figure 9 that high combustion-chamber discharge temperatures should be used. High thrust is the more important consideration in take-off, climb, and maximum-speed operation.

The curves of figure 9 show that, with no limitation on

compressor pressure ratio, higher thrust per unit mass rate of air flow and lower specific fuel consumption can be obtained by increasing the combustion-chamber outlet temperature until the value giving minimum specific fuel consumption is reached. For figures 9(a), 9(b), and 9(c), this temperature is less than 1460° R, about 2210° R, and 1710° R, respectively. Further increase in temperature permits an increase in thrust at the cost of increase in specific fuel consumption. As the gas temperature at the combustion-chamber outlet is increased, a large increase in compressor pressure ratio is required to maintain nearly minimum specific fuel consumption.

If the available compressor pressure ratio is limited, the combustion-chamber outlet temperature for minimum specific fuel consumption is very sensitive to the other operating conditions. For example, at a limiting compressor pressure ratio of 4, minimum specific fuel consumption occurs at a temperature below the lowest values shown in figure 9. If the limiting compressor pressure ratio is 8, the combustion-chamber discharge temperature for minimum specific fuel consumption is still less than the lowest temperature shown in figure 9(c) for an atmospheric temperature of 412° R but approaches an intermediate value of approximately 1710° R for an atmospheric temperature of 519° R (fig. 9(b)). The optimum combustion-gas temperature is also very sensitive to the efficiencies of the components of the jet-propulsion units.

In figure 10(a) the specific fuel consumption and the thrust per unit mass rate of air flow are plotted against airplane velocity for the conditions listed in the figure for the following cases:

(a) Compressor pressure ratio chosen to give values of A = 1

(b) Compressor pressure ratio chosen to give minimum specific fuel consumption

It is noted that the specific fuel consumption for case (a) is between 15 and 23 percent higher than for case (b) for airplane velocities between 300 and 800 feet per second; the percentage difference in specific fuel consumption is greater at the lower airplane velocities and at the lower atmospheric temperatures.

The thrust per unit mass rate of air flow is between 21 and 31 percent higher for case (a) than for case (b) for air-

plane velocities between 300 and 800 feet per second; the greater percentage difference in thrust per unit mass rate of air flow occurs at the lower airplane velocities and the lower atmospheric temperature.

Figure 10(b) shows the compressor pressure ratios and the values of A that are associated with the performance values given in figure 10(a). The large increase in required pressure ratio from the condition of $A = 1$ to the condition of minimum specific fuel consumption is noted.

In figures 8, 9 and 10 it was assumed that the compressor efficiency remains constant at 85 percent regardless of pressure ratio. As the desired pressure ratio is increased, however, it becomes increasingly difficult to design the compressor to maintain a high efficiency and a reduction in compressor efficiency may be expected. The reduction in the obtainable compressor efficiency with increase in pressure ratio will reduce the gains derived from increase in pressure ratio and hence will reduce the value of the optimum pressure ratio.

This condition will be illustrated by consideration of a turbojet engine equipped with a multistage axial flow compressor each stage of which provides a pressure ratio of 1.25 at an efficiency η_c of 88 percent. The other parameters of the turbojet engine are the same as for figure 9(b). Figure 11 shows the over-all efficiency of the compressor, the thrust per unit mass rate of air flow, and specific fuel consumption of the engine plotted against pressure ratio. The pressure ratio is increased by adding stages to the compressor. It is noted that although the efficiency per stage was held constant the over all compressor efficiency decreases with increase in pressure ratio. At a pressure ratio of 5 the compressor efficiency is 88 percent, the value used in the computation for figure 9. Dotted on figure 11 are curves taken from figure 9(b). For the range of combustor outlet temperatures T_4 shown, the values of compressor pressure ratios for maximum $F/\dot{m}$ and minimum W_f/F are lower for the case when the reduction in compressor efficiency with increased pressure ratio is considered than those for the case of constant compressor efficiency of 85 percent. This change in pressure ratios is more pronounced at the higher values of T_4.

Figure 11 pertains to the increase in pressure ratio by an increase in the number of stages. In a turbojet engine with a given compressor an increase in pressure ratio is obtained by an increase in rotational speed which, at high rotational speeds, is usually accompanied by a reduction in compressor

efficiency. This case will be discussed in greater detail later.

The effect of the increase in pressure ratio on turbine efficiency is a more complex matter and will not be considered in detail here. An increase in the number of turbine stages with a constant pressure ratio and efficiency per stage will result in an increase in over all turbine efficiency. There will be a tendency, however, to design for increased pressure ratio per stage in addition to increasing the number of stages when increased over all pressure ratios are desired, in order to economize on the size and weight of the turbine. Operation at increased pressure ratio per stage may result in some reduction in turbine efficiency per stage which may offset gains obtained from the increased number of stages. The net effect on the over-all turbine efficiency will depend on the compromise between pressure ratio per stage and number of stages decided upon.

The points on the curves of figures 9 to 11 relate to a series of turbojet engines in which the components are changed to provide the desired characteristics at each point. It is of some interest to examine over a variety of operating conditions the characteristics of a turbojet engine having a given turbine and compressor.

The performance characteristics of the engine will depend on the performance characteristics of the particular compressor, combustion chamber, and turbine chosen, however, the essential trends may be brought out by a consideration of several illustrative cases. The characteristics of a typical turbine, centrifugal compressor, and axial flow compressor will be shown followed by plots of the performance characteristics of two turbojet engines incorprating these components, the first engine utilizing the centrifugal compressor and the second utilizing the axial flow compressor. The characteristics of the components to be discussed are purely illustrative and are not to be interpreted as indicative of the best performance obtainable. The discussion will be simplified by neglecting the weight of fuel in considering the turbine output and by assuming that the pressure drop through the combustor is proportional to the combustor inlet pressure. The errors introduced by these simplifications are sufficiently small so as not to influence the basic trends to be illustrated. In the computation of the performance of the illustrative turbojet engines the following parameters are assumed:

Discharge velocity coefficient C_v	0.97
Combustion efficiency η_f	.96
Heating value of fuel h_f, Btu/lb	18900
ϵ	1.00

Figure 12 shows the performance characteristics of a typical single stage turbine of low reaction. The mass flow of gas through the turbine is presented in figure 12(a) by a plot of $M_t\sqrt{\theta_4}/\delta_4$ against p_4/p_{5s}. The values of the upper abscissa $V_t/\sqrt{\theta_4}$, corresponding to the values of p_4/p_{5s} are obtained from the velocity equation

$$V_t = \sqrt{2J\, c_p\, T_4 \left[1 - \left(\frac{p_{5s}}{p_4}\right)^{\frac{\gamma-1}{\gamma}}\right]}$$

The values of the ordinate M_tV_t/δ_4 are obtained by taking the product of $M_t\sqrt{\theta_4}/\delta_4$ and $V_t/\sqrt{\theta_4}$. Above a pressure ratio of 2.5 across the turbine the value of $M_t\sqrt{\theta_4}/\delta_4$ is constant (i.e. choking occurs at the turbine nozzle).

The turbine efficiency η_t as shown in figure 12(b) is principally a function of the turbine blade to theoretical turbine jet velocity u/V_t and to a much lesser extent a function of the pressure ratio and flow Reynolds number. The blade speed u is measured along the blade pitch circumference. The turbine jet velocity V_t is defined as the theoretical jet velocity developed by a gas expanding ideally through the turbine nozzle from turbine inlet total temperature and pressure to turbine discharge static pressure. Curves for η'_t are also shown in figure 12(b). The turbine efficiency η'_t is defined as

$$\eta'_t = \frac{\text{Turbine shaft power}}{\frac{1}{2} M_t V_t^2} \qquad (6)$$

where M_t is the mass flow of gas through the turbine and hence $\frac{1}{2} M_t V_t^2$ is the theoretical kinetic energy available for work.

In this definition the turbine is not credited with the kinetic energy corresponding to the average axial velocity of the gas at the turbine exit.

In compressor practice it is convenient to define a quantity K_c (called the slip factor) as follows:

$$K_c = \frac{\text{Compressor power}}{\dot{M}U^2} \tag{7}$$

where U is the compressor tip speed and $\dot{M}$ is the mass rate of air flow through the compressor. The quantity K_c for a centrifugal compressor is usually somewhat less than unity and does not vary appreciably with change in operating conditions.

In a turbojet engine the compressor power is equal to the turbine power hence from equations (6) and (7)

$$K_c U^2 = \frac{1}{2} V_t^2 \eta_t' \tag{8}$$

(The difference between $\dot{M}$ and $\dot{M}_t$ has been neglected). If B is defined as the ratio of the compressor tip speed U to the turbine blade speed u and hence is a constant for any given turbojet engine, equation (8) becomes

$$K_c B^2 = \frac{1}{2}\left(\frac{V_t}{u}\right)^2 \eta_t' \tag{9}$$

Because η_t' is a function primarily of u/V_t, the value of u/V_t and hence η_t' and η_t are determined by the value of K_c. When K_c is known the value of $\sqrt{\eta_t'}/(u/V_t)$ is evaluated from equation (9), then using figure 12(b) the values of u/V_t, η_t', and η_t are found. For a compressor for which K_c is nearly constant (for example the centrifugal compressor) the turbine will operate at nearly constant blade to jet speed ratio and hence nearly constant turbine efficiency over the entire operating range of the engine.

Figure 13 shows the conventional presentation of performance curves for a typical centrifugal compressor. The compressor pressure ratio p_2/p_1, adiabatic efficiency η_c, and slip factor K_c, are plotted against the mass flow factor $\dot{M}\sqrt{\theta_1}/\delta_1$, for various values of the tip speed factor $U/\sqrt{\theta_1}$.

By increasing the tip speed both the pressure ratio and mass flow can be increased, the compressor efficiency, however, decreasing. At a given tip speed a reduction in mass flow by throttling the compressor outlet results in an increase in pressure ratio and efficiency to peak values. Stalling of the compressor accompanied by surging of the flow occurs at excessive throttling at the positions indicated by the dot-dashed surge line.

Over the operating range of the compressor the value of the slip factor K_σ varies between .80 and 1.00. The corresponding turbine efficiencies obtained from figure 12(b) and equation (9) are shown plotted in figure 13 for various values of K_σ. The value of η_t is substantially constant over the entire range of operation as shown in figure 13.

Dotted lines representing constant ratio of turbine inlet to compressor inlet temperature T_4/T_1 are also shown in figure 13. These lines are obtained as follows: When the difference between M and M_t is neglected,

$$\frac{M\sqrt{T_1}}{p_1} = \frac{p_4}{p_1}\sqrt{\frac{T_1}{T_4}}\ \frac{M_t\sqrt{T_4}}{p_4}$$

Let r represent the ratio of the combustor pressure drop to the combustor inlet pressure, i.e.

$$p_2 - p_4 = r\,p_2$$

or

$$p_4 = (1-r)p_2$$

Hence

$$\frac{M\sqrt{T_1}}{p_1} = (1-r)\ \frac{p_2}{p_1}\sqrt{\frac{T_1}{T_4}}\ \frac{M_t\sqrt{T_4}}{p_4}$$

or

$$\frac{M\sqrt{\theta_1}}{\delta_1} = (1-r)\ \frac{p_2}{p_1}\sqrt{\frac{T_1}{T_4}}\ \frac{M_t\sqrt{\theta_4}}{\delta_4} \qquad (10)$$

At high rotor speeds of the turbojet engine where choking of the flow at the turbine nozzle occurs, the value of $M_t\sqrt{\theta_4}/\delta_4$ becomes constant. (For example in the region of pressure ratios p_4/p_{5s} above 2.5 for the turbine shown in figure 12(a)). When this value of $M\sqrt{\theta_4}/\delta_4$ is substituted into equation (10) and a value is assumed for r it is possible from this equation to compute the value T_4/T_1 for desired design values of $M\sqrt{\theta_1}/\delta_1$ and p_2/p_1. In the non-choking zone the value of $M\sqrt{\theta_4}/\delta_4$ is not so easily determined and the more

general method described in appendix B may be used.

Every point in figure 13 is a possible operating point provided that the turbojet engine is equipped with a variable area discharge nozzle. At any given rotative speed and compressor inlet temperature T_1, increasing the combustor outlet temperature T_4 is equivalent to throttling the compressor. This causes an increase in compressor pressure ratio and adiabatic efficiency until a peak value is reached. Excessive combustor outlet temperature will carry operation past peak conditions to surging.

When the engine is provided with a fixed discharge nozzle then for any given flight Mach number, operation at any one tip speed factor $U/\sqrt{\theta_1}$ is limited to one value of T_4/T_1. Figure 13 shows for an illustrative nozzle area A_n the lines of operation at $Y = 0$ and $Y = 0.1$ (the method used to determine these lines is described in appendix C). In the region of high rotative speeds the jet velocity V_j becomes supersonic so that the discharge nozzle is choked and the curves for various values of Y merge into a single curve. For a constant discharge nozzle area at any given value of Y and compressor inlet temperature T_1, as the combustion chamber discharge temperature T_4 is reduced the compressor tip speed decreases and operation at a reduced compressor pressure ratio must be accepted.

Figure 14 shows the thrust factor F/δ_1, the thrust per unit mass rate of air flow factor $F/W\sqrt{\theta_1}$, and the specific fuel consumption factor $W_f/F\sqrt{\theta_1}$, of the turbojet engine corresponding to the conditions shown in figure 13 for values of Y of 0 and 0.1, (i.e. flight Mach numbers of 0 and 0.707 respectively).

The thrust factor and thrust per unit mass rate of air flow factor are seen to increase appreciably with increase in T_4/T_1. The thrust per unit mass rate of air flow factor for a constant T_4/T_1 remains almost constant or decreases with increase in $U/\sqrt{\theta_1}$. This is a consequence of the reduction in compressor efficiency which offsets the effect of increased pressure ratio p_2/p_1 when $U/\sqrt{\theta_1}$ is increased. The thrust factor, however, increases appreciably with $U/\sqrt{\theta_1}$ because of the attending increase in the mass flow factor. Every point on this figure 14 is a possible operating point if the engine is provided with a variable area discharge nozzle. A line of constant nozzle area is also shown in this figure.

The lowest value of the specific fuel consumption factor in figure 14 is obtained at a $U/\sqrt{\theta_1}$ of about 1350 ft/sec and a T_4/T_1 of about 3. When operation is limited to the constant discharge nozzle area line it is found that for Y = 0.1 (fig. 14(b)), the specific fuel consumption factor is increasing as the value of T_4/T_1 is decreasing to 3 (the minimum value of $W_f/F\sqrt{\theta_1}$ occurring at a T_4/T_1 of about 3.7). Hence the desirability of a variable area discharge nozzle is apparent.

The occurance of minimum $W_f/F\sqrt{\theta_1}$ at an intermediate turbine inlet temperature was anticipated from figure 9. The large reduction of compressor efficiency with increase in compressor tip speed at the range of high $U/\sqrt{\theta_1}$ (see fig. 13) resulted in the location of the point of minimum specific fuel consumption factor in the range of intermediate tip speeds. For any given tip speed factor it is noted in figure 13 that operation at T_4/T_1 of 3 occurs at a lower p_2/p_1 and lower η_c than operation at T_4/T_1 of 4. If low specific fuel consumption were the primary objective of the design, then by choosing a turbine of smaller nozzle area it would be possible to move the location of the $T_4/T_1 = 3$ line in figure 13 to the position of the $T_4/T_1 = 4$ line and realize at $T_4/T_1 = 3$ an improvement in specific fuel consumption resulting from the increased pressure ratio and compressor efficiency. In this case operation at the high values of T_4/T_1 will be displaced into the surge zone and some reduction in maximum thrust of the engine will result. Hence to obtain the ultimate in both specific fuel consumption and thrust from a given engine a variable turbine nozzle area as well as a variable area discharge nozzle would be beneficial.

Figure 15 shows the performance characteristics of a typical axial flow compressor. Comparison of figures 15 and 13 shows the difference in characteristics between the axial flow and centrifugal compressors. At high tip speeds, operation at any given tip speed is limited to a much narrower range of mass flow for the axial flow than for the centrifugal flow compressor. Hence, the turbine flow area must be designed with greater accuracy for the axial flow than for the centrifugal compressor to obtain a proper match of turbine and compressor characteristics at the design point.

The curve of compressor efficiency for a tip speed factor of 990 ft/sec is almost constant over the limited range of pressure ratios shown in figure 15 for this speed; that is over

the pressure ratio range from 2.8 to 3.4. Outside this pressure ratio range the efficiency may drop sharply. The shapes of these curves are very sensitive to the details of the compressor design and the blade angle settings. The axial flow compressor shows less loss in efficiency than the centrifugal compressor with increase in pressure ratio in the range shown. The axial flow compressor has the advantage over the single stage centrifugal compressor in that it can be designed for any desired pressure ratio by providing sufficient stages to insure good stage efficiencies. For the centrifugal compressor, an increase in pressure ratio is obtained by an increase in tip speed and hence velocities at the impeller exit which are in the transonic and supersonic ranges are eventually involved. This gives rise to the problem of efficiently converting these velocities into pressure in the diffuser.

The variation of the factor K_c is much greater for the axial flow than for the centrifugal compressor. At the high tip speeds, however, the variation in K_c for the axial flow compressor is sufficiently limited in the interesting operating range as to provide nearly constant turbine efficiency. The turbine efficiency curves in figure 15 were obtained from figure 12 and equation (9) and relate to a turbojet engine incorporating the turbine and axial flow compressor characterized by the data in figures 12 and 15 respectively.

The lines of constant T_4/T_1 for this engine were computed in the manner described in appendix B from the data of figures 12 and 15. The lines for an illustrative constant nozzle area A_n are also shown.

The thrust factor, thrust per unit mass rate of air flow factor, and specific fuel consumption factor, are shown in figure 16 for the turbojet engine corresponding to the data of figure 15. The minimum value of the specific fuel consumption factor in figure 16 is obtained at a value of T_4/T_1 of 3 and occurs at the highest tip speed factor shown. The fact that compressor efficiency does not fall off with increase in tip speed in the range shown contributes to the occurance of minimum $W_f/F\sqrt{\theta_1}$ at the high $U/\sqrt{\theta_1}$. It should be noted that the curves for the axial flow compressor do not cover as high a range of pressure ratios as the curves for the centrifugal compressor, figures 13 and 14.

Figures 13 and 14 or 15 and 16 for a turbojet engine with a constant discharge nozzle area indicate that for a constant flight Mach number (constant value of Y) the factors F/δ_1, $M\sqrt{\theta_1}/\delta_1$, $F/M\sqrt{\theta_1}$, T_4/T_1, and $W_f/F\sqrt{\theta_1}$, each should plot as a single curve against $U/\sqrt{\theta_1}$, regardless of the altitude of operation (i.e. regardless of atmospheric pressure and temperature). This is found to be true in practice except for the specific fuel consumption factor. In this case, the assumptions of a constant combustion efficiency and a given specific heat of gases during combustion for a given T_4/T_1, do not hold in actual operation.

The performance of the two illustrative turbojet engines presented herein are not indicative of the best performance obtainable with this type of engine because no attempt was made to pick components of optimum characteristics. It was hoped, however, that the discussion of these illustrative engines would provide some insight into the manner in which the performance characteristics of the components influenced the performance of the engine, and some understanding of the basic characteristics and limitations of this type of engine.

APPENDIX A

EQUATIONS FOR THE PERFORMANCE FIGURES

The equation numbers correspond to those in the derivation given in appendix C, reference 6.

Figure 2:

$$Y = \frac{V_o^2}{2\,J\,c_{pa}\,T_o} = \frac{1}{2\,J\,c_{pa}\,519}\left(V_o\sqrt{\frac{519}{T_o}}\right)^2 \qquad (C6)$$

$$\frac{p_1 + \Delta p_d}{p_o} = \left[1 + \frac{1}{2\,J\,c_{pa}\,519}\left(V_o\sqrt{\frac{519}{T_o}}\right)^2\right]^{\frac{\gamma_a}{\gamma_a - 1}} \qquad (C70)$$

$$\text{Flight Mach number} = \sqrt{\frac{1}{(\gamma_a - 1)\,J\,c_{pa}\,519}}\left(V_o\sqrt{\frac{519}{T_o}}\right) \qquad (C72)$$

Figure 3:

$$\frac{p_2}{p_1} = \left(1 + \frac{\eta_c\,Z}{1 + Y}\right)^{\frac{\gamma_a}{\gamma_a - 1}} \qquad (C67)$$

$$\left(\frac{p_2}{p_1}\right)_{ref} = \left[\left(\frac{1}{1 + Y}\right)^2 \eta_c\eta_t \in \frac{T_4}{T_o}\right]^{\frac{\gamma_a}{2(\gamma_a - 1)}} \qquad (C68)$$

Figure 4(a):

$$V_j\sqrt{\frac{\eta_c\eta_t}{C_v^2}\frac{519}{T_o}} = \sqrt{\frac{519}{T_o}\,V_o^2 + 2Jc_{pa}519\left[\eta_c\eta_t\in\frac{T_4}{T_o} - \left(A' + \frac{1}{A'}\right)\left(\sqrt{\eta_c\eta_t\in\frac{T_4}{T_o}} + 1\right)\right]} \qquad (C37)$$

where $A' = A^{\frac{\gamma_a - 1}{\gamma_a}}$

Figure 4(b):

$$\frac{\Delta V_j}{V_j} = \frac{\frac{1}{2}\left[1 - \left(\frac{C_v V_5}{V_j}\right)^2\right]\left(\frac{1}{\eta_t} - 1\right)}{\frac{T_4}{T_o}\,Z\,\frac{c_p}{c_{pa}} - 1} \qquad (C62)$$

Figure 5:

$$T_2 = \frac{c_{pa}}{c_{pa2}}\, T_o\,(1 + Y + Z) \qquad (C29)$$

Figure 6:

$$\eta_f f = \frac{\bar{c}_p\,(T_4 - T_2)}{32.2\ h} \qquad (C27)$$

where $\bar{c}_p$ is determined from reference 8

Figure 7(a):

$$a = \frac{\Delta p_d}{p_o}\left(\frac{\gamma_a - 1}{\gamma_a}\right)\frac{1}{Y + \eta_c Z} \qquad (C43)$$

Figure 7(b):

$$b = \frac{\Delta p_{(2-4)}}{p_o}\left(\frac{\gamma_a - 1}{\gamma_a}\right)\frac{1}{Y + \eta_c Z}\left(\frac{1}{1 + Y + \eta_c Z}\right)^{\frac{\gamma_a}{\gamma_a - 1}} \qquad (C45)$$

Figure 7(c):

$$c = \frac{\left(W_{th}/R\,T_4\right)}{\left(\frac{\gamma_a}{\gamma_a - 1}\right)\left[1 - \left(\frac{p_o}{p_2}\right)^{\frac{\gamma_a - 1}{\gamma_a}}\right]^{\frac{\gamma_a - 1}{\gamma_a}}}\,\frac{R}{R_a} - 1 \qquad (C50)$$

where values of W_{th}/RT_4 are obtained from reference 10.

Symbols used in these equations in addition to those given in the paper are:

c_p — average specific heat at constant pressure of the exhaust gases during the expansion process. This term, when used with the temperature change accompanying the expansion, gives the change in enthalpy per unit mass. (Btu)/(slug)($^\circ$F)

$\overline{c}_p$ — average specific heat at constant pressure of the gases during the combustion process. This term, when used with the temperature change during combustion, is used to determine the fuel consumption. (Btu)/(slug)($^\circ$F)

c_{pa} — specific heat of air at constant pressure at a T_c = 519° R, 7.73 (Btu)/(slug)($^\circ$F)

c_{pa2} — specific heat of air at constant pressure at compressor outlet total temperature. It is equal to the enthalpy per unit mass (zero enthalpy arbitrarily fixed at absolute zero temperature) divided by the total temperature. (Btu)/(slug)($^\circ$F)

R — gas constant of exhaust gas, (ft-lb)/(slug)($^\circ$F)

R_a — gas constant of air, (ft-lb)/(slug)($^\circ$F)

W_{th} — ideal work in a thermodynamic process, ft-lb/lb

APPENDIX B

The following is a procedure for plotting lines of constant T_4/T_1 on compressor characteristic curves such as figure 13 for a given turbojet engine.

Equation (8) may be written

$$K_c \frac{U^2}{\theta_1} = \frac{1}{2} \frac{V_t^2}{\theta_4} \eta'_t \frac{T_4}{T_1} \tag{11}$$

When T_4/T_1 is eliminated between equations (10) and (11) there results

$$\sqrt{K_c} \frac{M}{\delta_1} \sqrt{\theta_1} \frac{U}{\sqrt{\theta_1}} = (1-r) \frac{p_2}{p_1} \frac{M_t V_t}{\delta_4} \sqrt{\frac{\eta'_t}{2}} \tag{12}$$

The method of using equation (12) to obtain the constant T_4/T_1 lines will be illustrated for the turbojet engine with a centrifugal compressor.

1. Select a point on figure 13 at a value of $U/\sqrt{\theta_1}$ and of p_2/p_1 for which the value of T_4/T_1 is desired.

2. Read the corresponding values of $M\sqrt{\theta_1}/\delta_1$, K_c, and an approximate value of η_t from figure 13.

3. Corresponding to the approximate value of η_t pick an approximate value of η'_t from figure 12 and compute an approximate value of u/V_t from equation (9).

4. For a given value of r compute the approximate value of $M_t V_t/\delta_4$ from equation (12).

5. Read from figure 12(a) the value $V_t/\sqrt{\theta_4}$ corresponding to the values of $M_t V_t/\delta_4$ and u/V_t previously obtained and from the same figure read $M_t\sqrt{\theta_4}/\delta_4$.

6. Compute T_4/T_1 from equation (10). This is a first approximation and in most cases is sufficiently accurate.

7. To evaluate a second approximation of T_4/T_1 first compute a new value of u/V_t from the identity

$$\frac{u}{V_t} = \frac{U/\sqrt{\theta_1}}{BV_t/\sqrt{\theta_4}} \sqrt{\frac{T_1}{T_4}}$$

8. Determine a new value of η_t' from figure 12 corresponding to the new value of u/V_t and the value of $V_t/\sqrt{\theta_4}$. (the latter factor is used to find p_4/p_{5s}).

9. Repeat steps (4), (5), and (6).

APPENDIX C

The following is the method for locating the operating lines of a turbojet engine equipped with a constant exhaust nozzle area, such as are shown in figure 13.

The jet velocity can be expressed as

$$V_j = C_v \sqrt{2Jc_p T_5 \left[1 - \left(\frac{p_o}{p_5}\right)^{\frac{\gamma-1}{\gamma}}\right]}$$

where T_5 is the total temperature at turbine discharge, $^{\circ}R$

p_5 is the total pressure at turbine discharge, (lb/sq ft absolute)

from which

$$\frac{V_j}{\sqrt{\theta_5}} = C_v \sqrt{2Jc_p\, 519 \left[1 - \left(\frac{p_o}{p_5}\right)^{\frac{\gamma-1}{\gamma}}\right]} \qquad (13)$$

The mass flow through the exhaust nozzle area is expressed as

$$W_t = A_n \rho_5 \left(\frac{p_o}{p_5}\right)^{\frac{1}{\gamma}} \sqrt{2Jc_p T_5 \left[1 - \left(\frac{p_o}{p_5}\right)^{\frac{\gamma-1}{\gamma}}\right]}$$

where ρ_5 is the stagnation density at turbine discharge, (slugs/cu ft)

Thus

$$\frac{W_t \sqrt{\theta_5}}{A_n \delta_5} = \frac{2116}{R\sqrt{519}} \left(\frac{p_o}{p_5}\right)^{\frac{1}{\gamma}} \sqrt{2Jc_p \left[1 - \left(\frac{p_o}{p_5}\right)^{\frac{\gamma-1}{\gamma}}\right]} \qquad (14)$$

This equation is used until the critical pressure ratio is reached. The value of the mass flow factor remains constant thereafter as p_o/p_5 becomes less than the critical pressure ratio.

From energy considerations

$$T_5 = T_4 - \frac{\eta_t' V_t^2}{2Jc_p}$$

from which

$$\frac{\theta_5}{\theta_4} = 1 - \frac{\eta'_t}{2Jc_p 519}\left(\frac{V_t}{\sqrt{\theta_4}}\right)^2 \qquad (15)$$

The jet velocity factor

$$\frac{V_j}{\sqrt{\theta_1}} = \frac{F}{M\sqrt{\theta_1}} - \frac{V_o}{\sqrt{\theta_1}}$$

which when using the definition for Y (see symbols) and equation (4) becomes

$$\frac{V_j}{\sqrt{\theta_1}} = \frac{F}{M\sqrt{\theta_1}} - \sqrt{2Jc_{pa}519\ \frac{Y}{1+Y}} \qquad (16)$$

The procedure for determining the design point nozzle area and the locus of the constant nozzle area curve is outlined below and illustrated for the case of a turbojet engine with a centrifugal compressor operating at Y = 0.1.

Determination of design nozzle area

1. Corresponding to the desired design point, chosen from a consideration of figures 13 and 14, read the values of p_2/p_1, $U/\sqrt{\theta_1}$, T_4/T_1, $M\sqrt{\theta_1}/\delta_1$, K_c, and an approximate value of η_t from figure 13, and the value of $F/M\sqrt{\theta_1}$ from figure 14(b).

2. Corresponding to the approximate value of η_t pick an approximate value of η'_t from figure 12(b) and compute an approximate value of u/V_t from equation (9).

3. For a given value of the ratio of combustor pressure drop to combustor inlet pressure, r, compute the approximate value of $M_t V_t/\delta_4$ from equation (12).

4. Read from figure 12(a) the value of $V_t/\sqrt{\theta_4}$ corresponding to the values of $M_t V_t/\delta_4$ and u/V_t previously obtained.

5. From $V_t/\sqrt{\theta_4}$, calculate θ_5/θ_4 using equation (15).

6. Calculate $V_j/\sqrt{\theta_1}$ using the values of $F/M\sqrt{\theta_1}$ and Y in equation (16).

7. From the identity

$$\frac{V_j}{\sqrt{\theta_5}} = \frac{V_1}{\sqrt{\theta_1}} \sqrt{\frac{\theta_4}{\theta_5}} \sqrt{\frac{T_1}{T_4}}$$

calculate $V_j/\sqrt{\theta_5}$. Using this value in equation (13) determine p_o/p_5.

8. Using the value of p_o/p_5 in equation (14) determine the mass flow factor $\frac{M_t\sqrt{\theta_5}}{A_n \delta_5}$. If the value of p_o/p_5 is less than the critical pressure ratio, then the same value of $\frac{M_t\sqrt{\theta_5}}{A_n \delta_5}$ as occurs at the critical pressure ratio is used.

9. Assuming a ram pressure loss, the value of p_1/p_o is evaluated.

10. A_n is then calculated from the identity

$$A_n = \frac{\left(\frac{M\sqrt{\theta_1}}{\delta_1}\right) \sqrt{\frac{T_4}{T_1}\frac{\theta_5}{\theta_4}}}{\left(\frac{M_t\sqrt{\theta_5}}{A_n \delta_5}\right) \left(\frac{p_5}{p_o}\right)\left(\frac{p_o}{p_1}\right)}$$

Determination of constant area curve

Once the design area has thus been found, the operational points of the engine with this constant exhaust nozzle area A_n have to be determined at other rotational speeds. At any given $U/\sqrt{\theta_1}$ the exhaust nozzle areas required for several operating points are determined by the method just outlined. The operating point corresponding to the design A_n at this given $U/\sqrt{\theta_1}$, is then determined by interpolation. This process is repeated for a sufficient range of values of $U/\sqrt{\theta_1}$, and the line of constant A_n located.

To obtain the operating line of constant A_n for another flight speed the procedure is repeated using the new value for Y.

It is noted that the difference between M and M_t was neglected in this procedure.

REFERENCES

1. Keirn, Col. D. J., and Shoults, D. R.: - Jet Propulsion and Its Application to High Speed Aircraft. Preprint of paper presented at I.A.S. meeting, August, 1945.

2. Bolz, Ray E.: - Graphical Solution for the Performance of Continuous-Flow Jet Engines. Preprint of paper presented at S.A.E. meeting, June, 1946.

3. Rubert, Kennedy F.: - An Analysis of Jet-Propulsion Systems Making Direct Use of the Working Substance of a Thermodynamic Cycle. NACA ACR No. L5A30a, 1945.

4. Palmer, Carl B.: - Performance of Compressor-Turbine Jet-Propulsion Systems, NACA ACR No. L5E17, 1945.

5. Hawthorne, William R.: - Factors Affecting the Design of Jet Turbines. Preprint of paper presented at S.A.E. meeting, January, 1946.

6. Pinkel, Benjamin, and Karp, Irving M.: - Performance Charts for a Jet-Propulsion System Consisting of a Compressor, a Combustion Chamber, and a Turbine. NACA ARR E6E14, 1946.

7. Keenan, Joseph H., and Kaye, Joseph: - Thermodynamic Properties of Air. John Wiley & Sons, Inc., 1945.

8. Turner, L. Richard, and Lord, Albert M.: - Thermodynamic Charts for the Computation of Combustion and Mixture Temperatures at Constant Pressure. NACA TN 1086, 1946.

9. Hicks, Bruce L.: - Addition of Heat to a Compressible Fluid in Motion. NACA ACR No. E5A29, 1945.

10. Pinkel, Benjamin, and Turner, L. Richard: - Thermodynamic Data for the Computation of the Performance of Exhaust-Gas Turbines. NACA ARR No. 4B25, 1944.

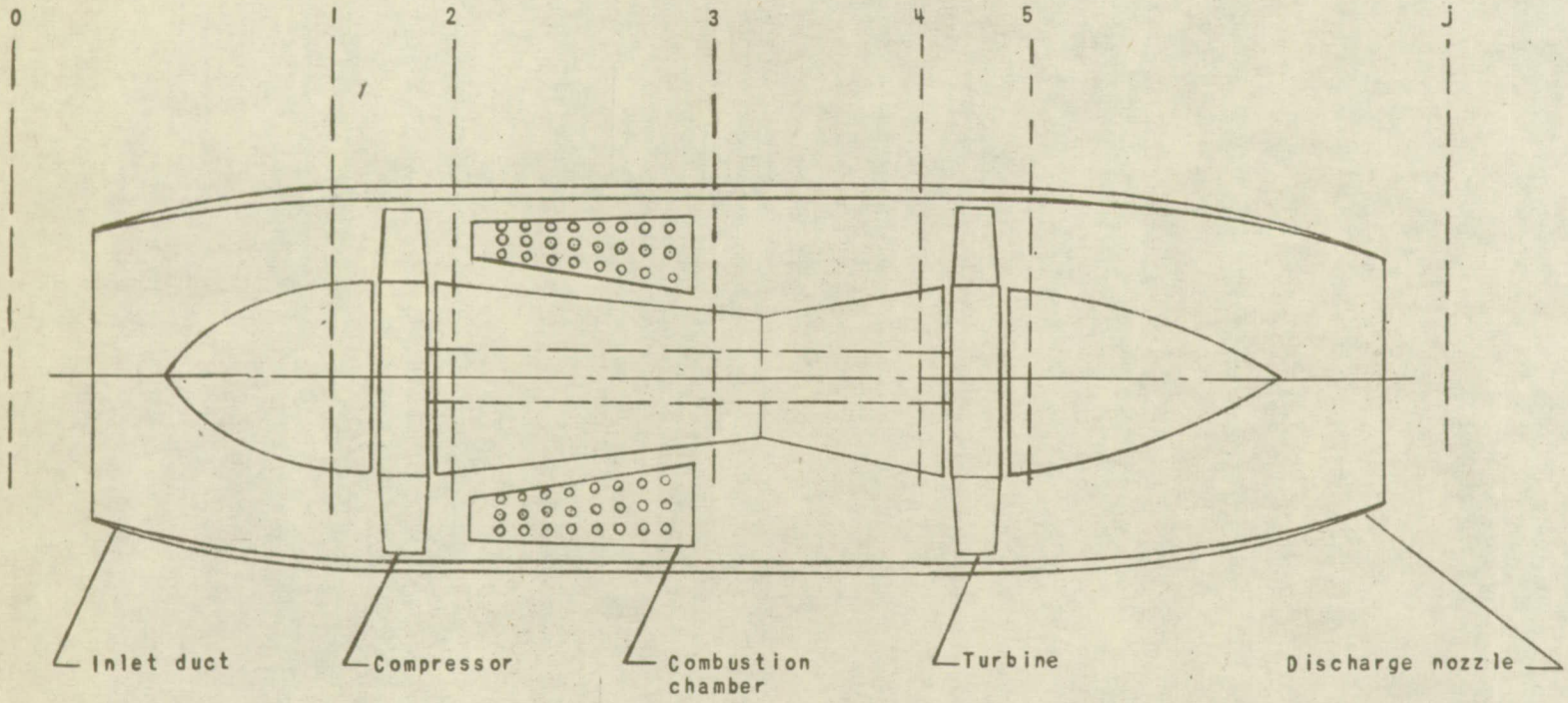

NATIONAL ADVISORY
COMMITTEE FOR AERONAUTICS

Figure 1. - Schematic diagram of the jet-propulsion system.

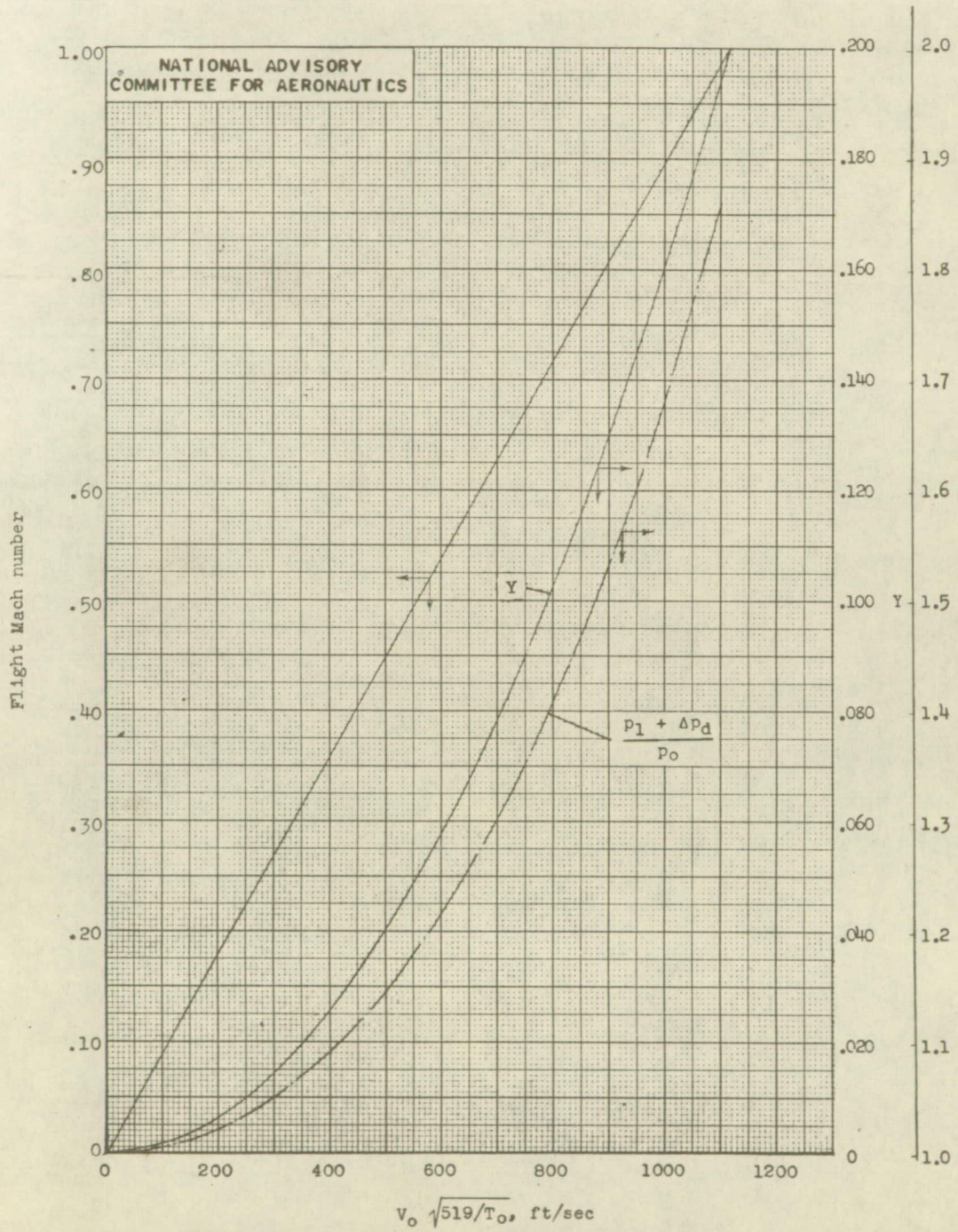

Figure 2.- Chart for determining Y, flight Mach number, and compressor inlet total pressure for various airplane velocities and atmospheric temperatures.

Fig. 3

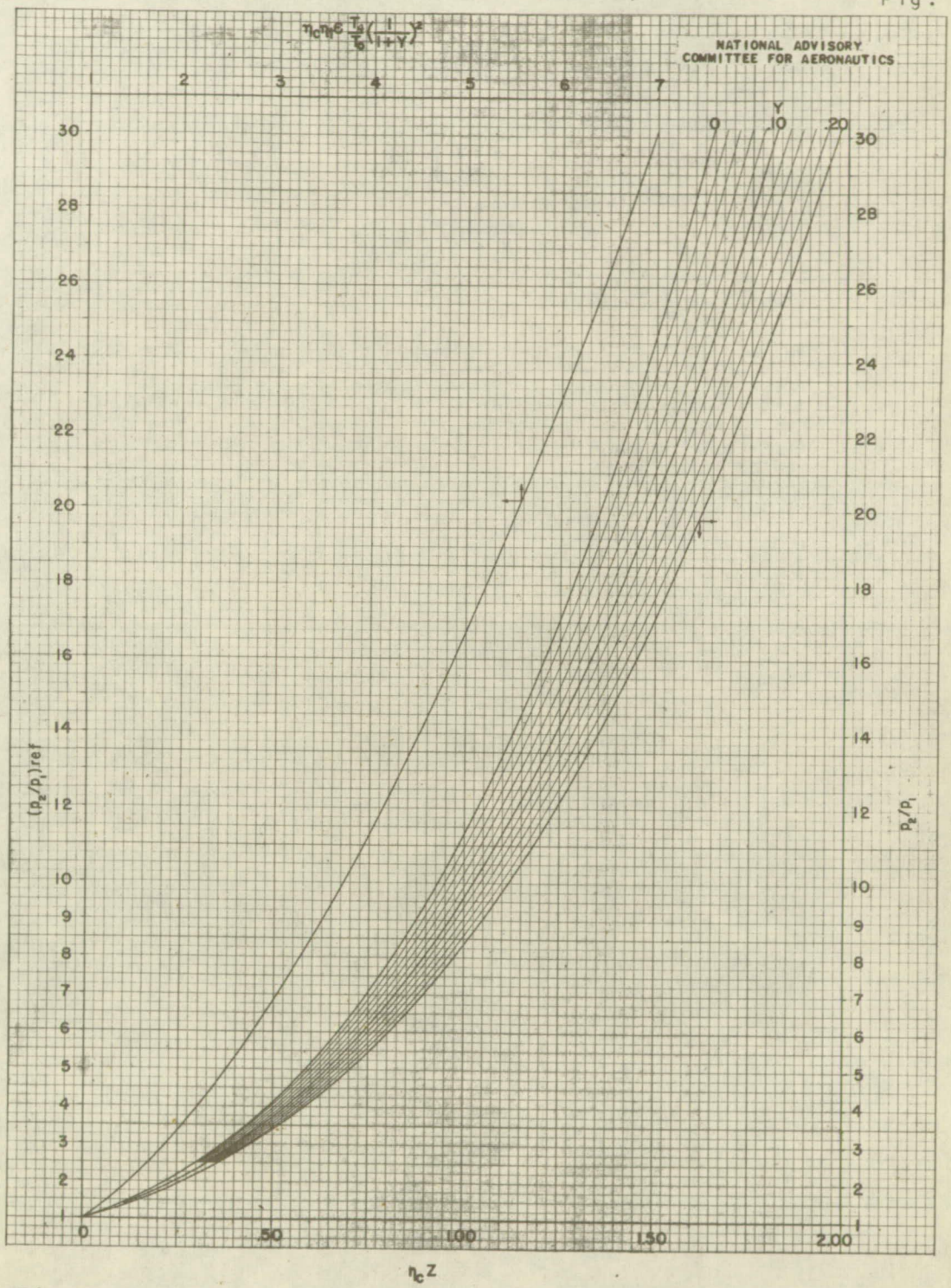

Figure 3. - Chart for determining the reference compressor pressure ratio for various values of $\eta_c\eta_t\xi\frac{T_4}{T_o}\left(\frac{1}{1+Y}\right)^2$ and the compressor pressure ratio for various values of Y and $\eta_c Z$.

Fig. 4a

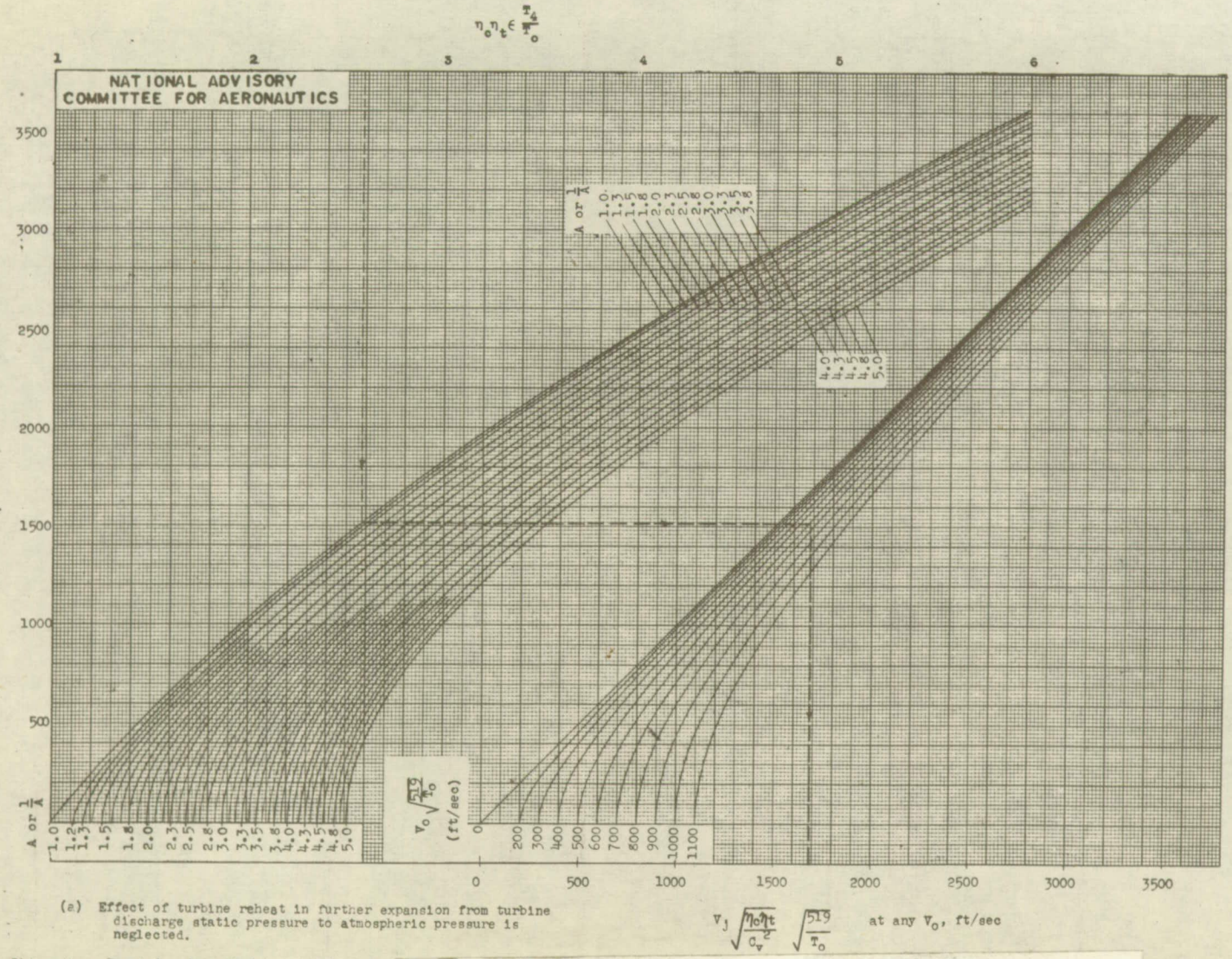

(a) Effect of turbine reheat in further expansion from turbine discharge static pressure to atmospheric pressure is neglected.

Figure 4. - Chart for determining jet velocity.

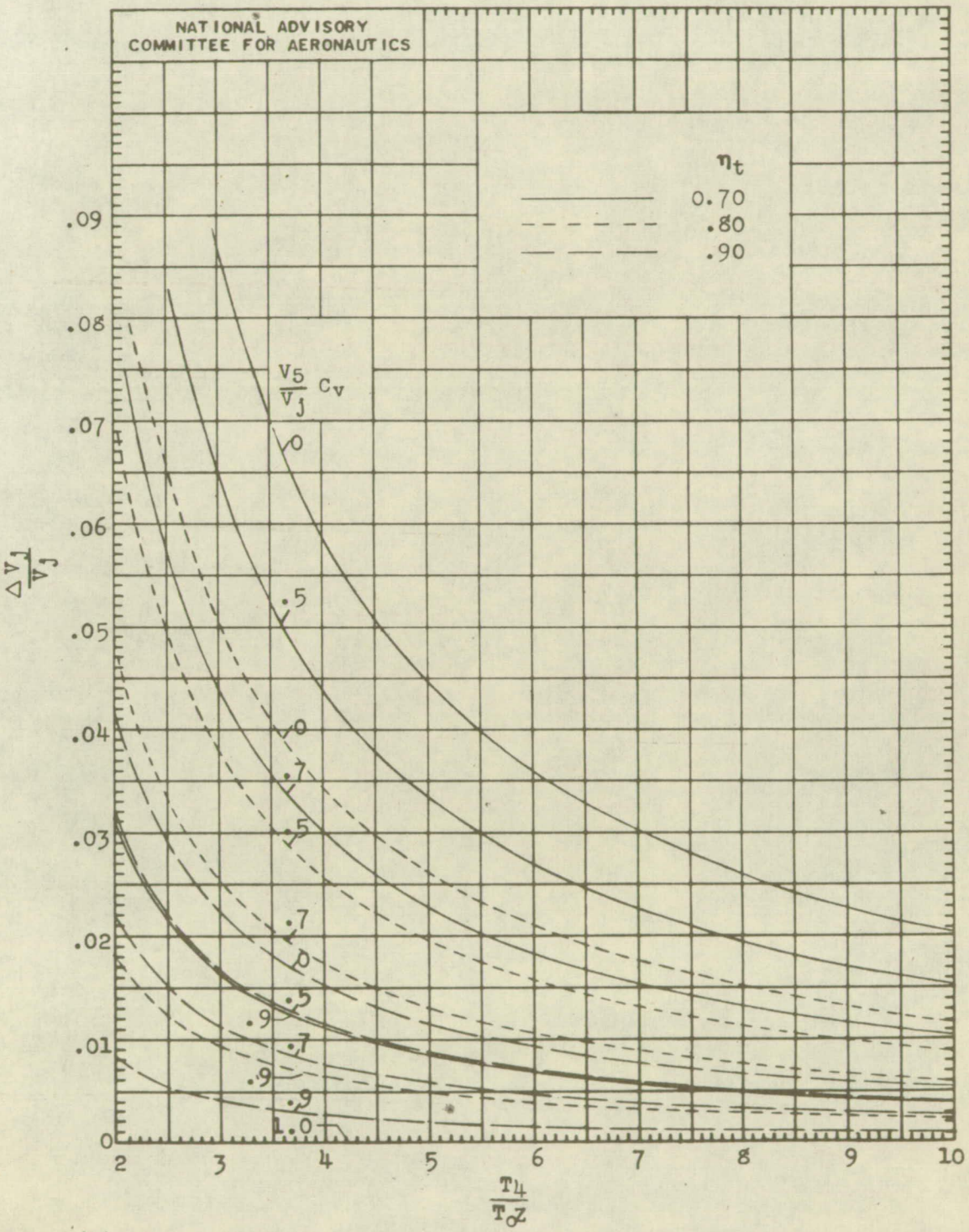

(b) Correction to jet velocity due to reheat in turbine.

Figure 4. - Concluded.

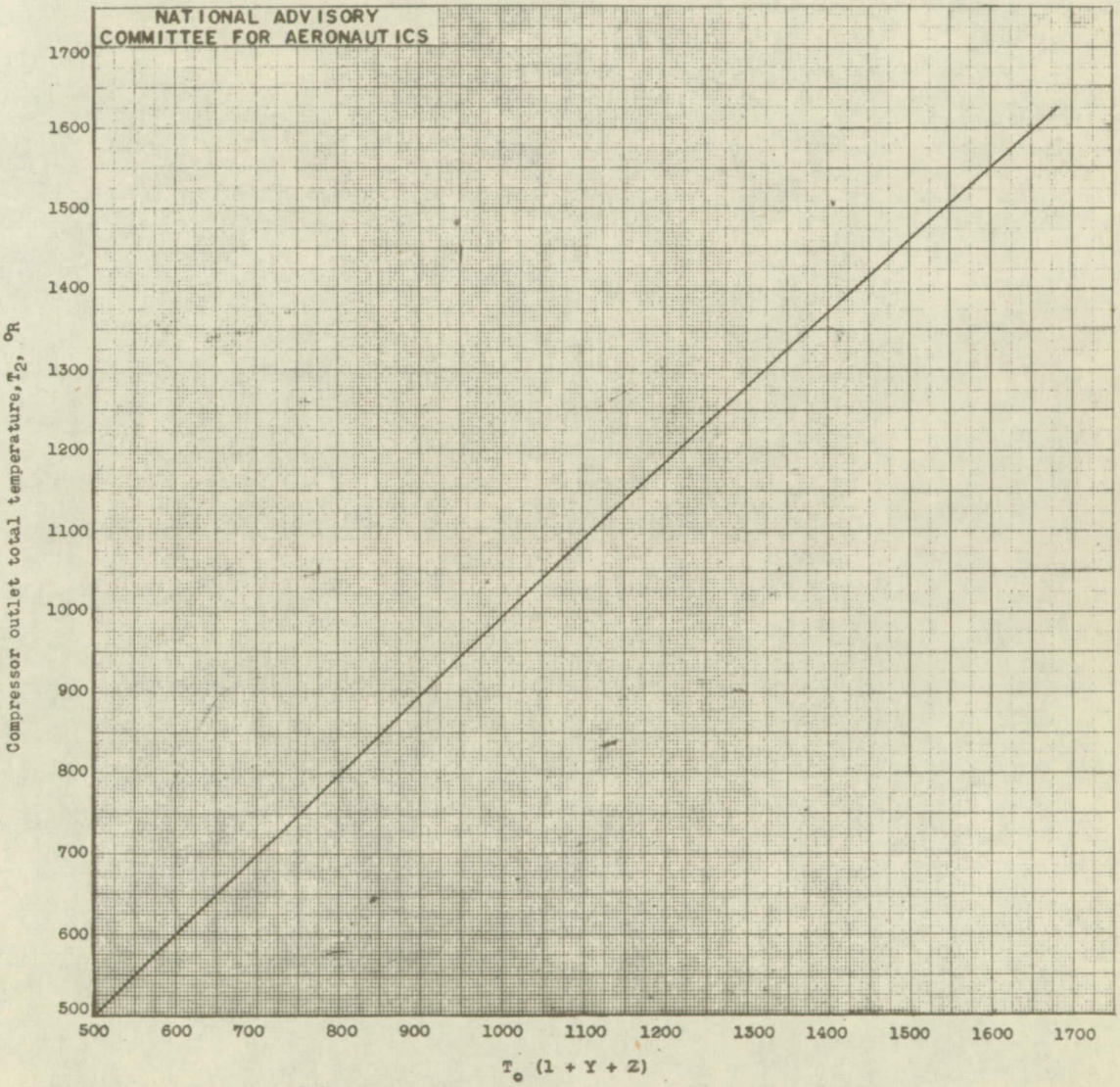

Figure 5. - Chart for determining the compressor outlet total temperature for various values of the factor T_o (1 + Y + Z).

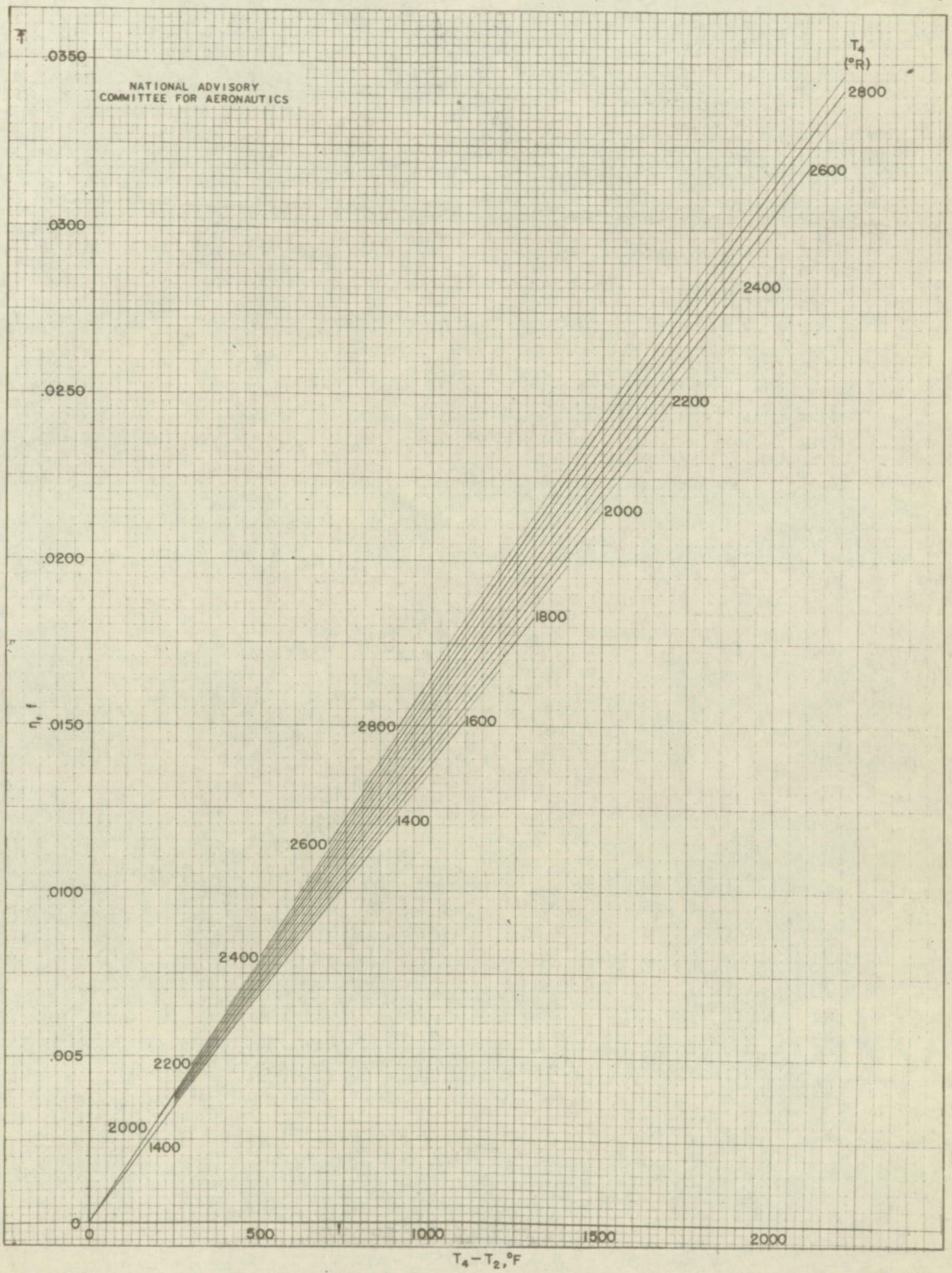

Figure 6. - Chart for determining the fuel-air ratio for various values of rise in total temperature across the combustion chamber and combustion chamber outlet total temperature. (h = 18,900 Btu/lb)

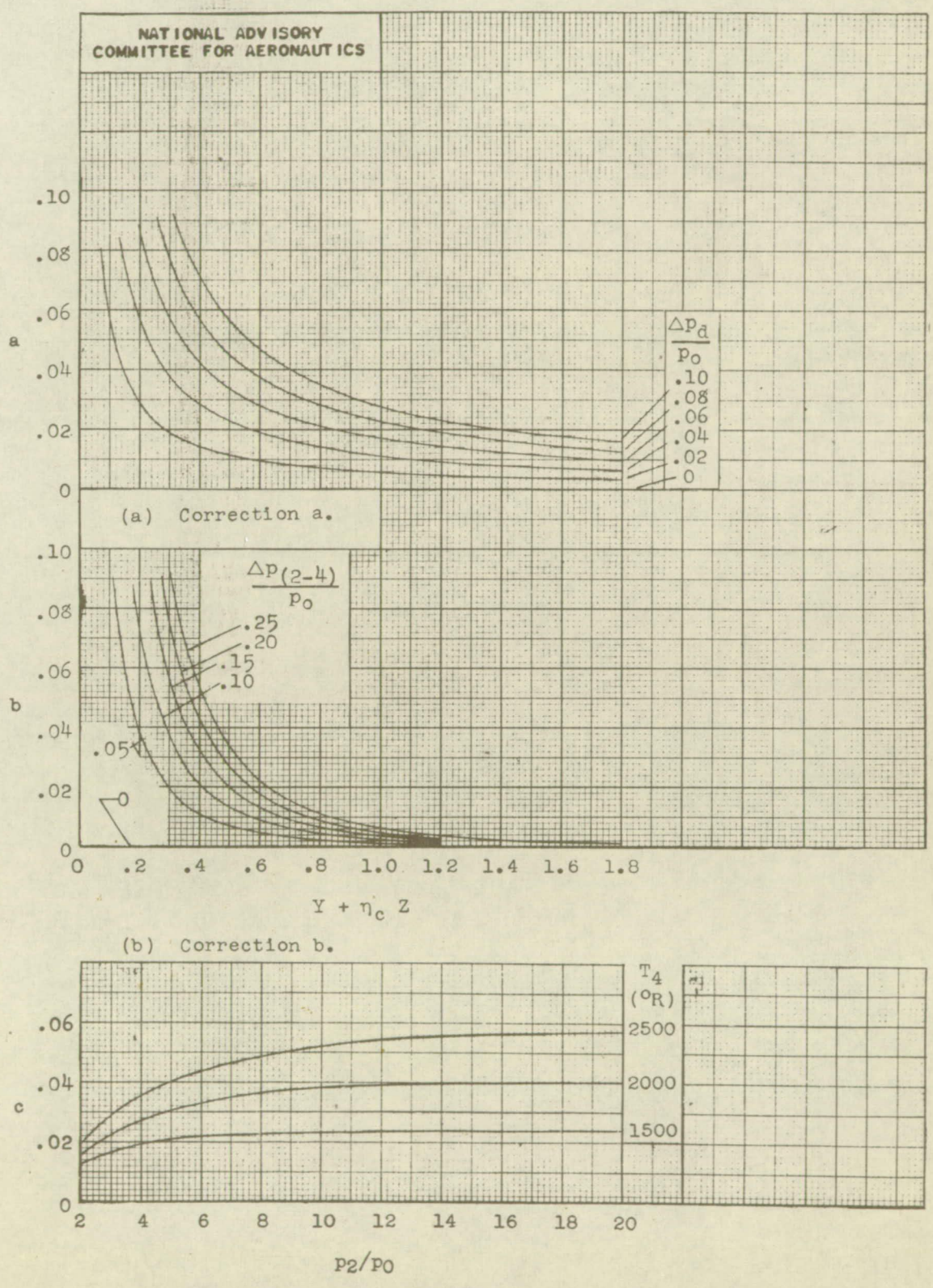

Figure 7.- Chart for determining the factor ϵ. ($\epsilon = 1-a-b+c$)

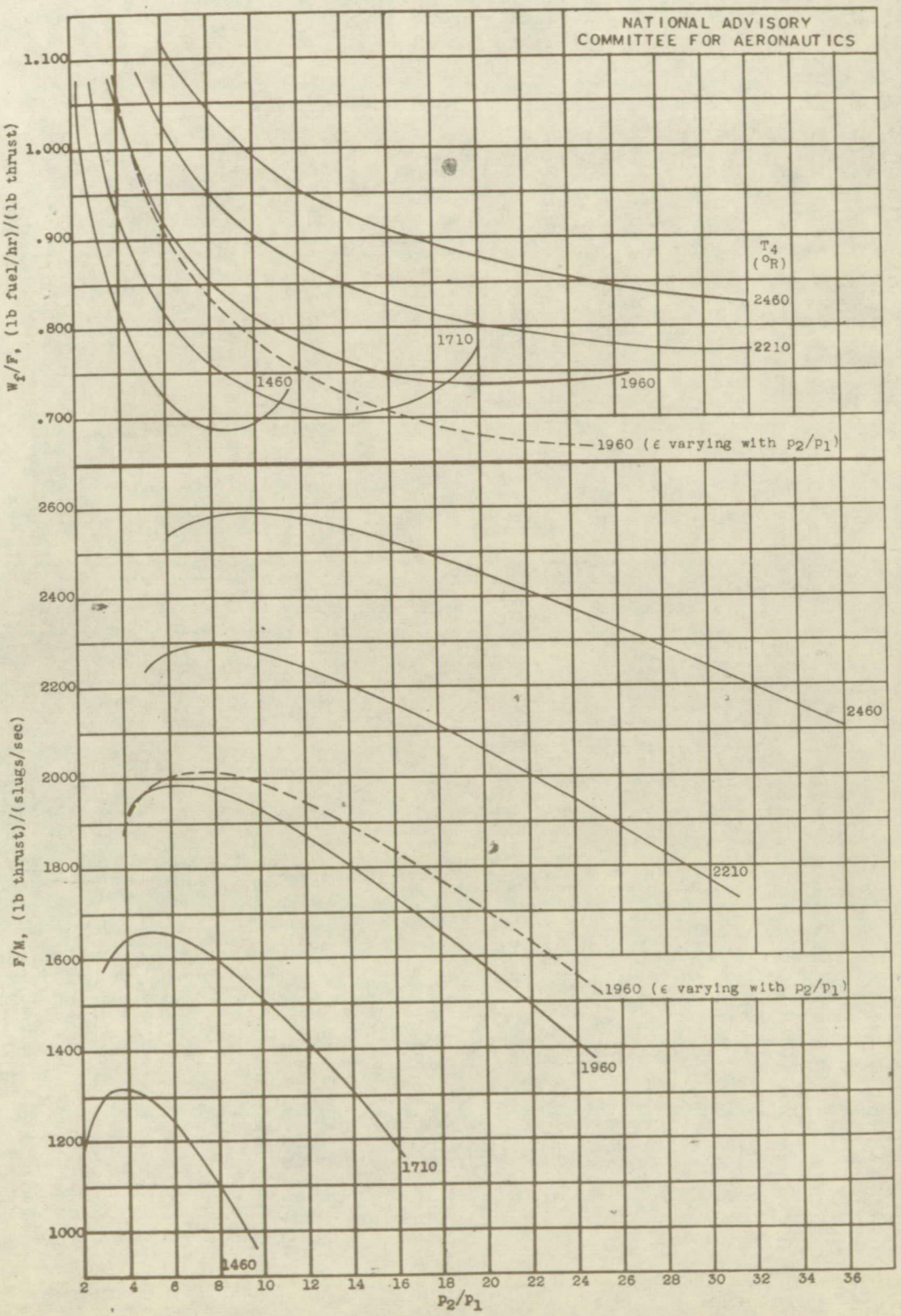

Figure 8. - Fuel rate per unit thrust and thrust per unit mass rate of air flow for various compressor pressure ratios and combustion-chamber discharge temperatures for illustrative case. (V_o, 0 ft/sec; T_o, 519° R; η_c, 0.85; η_t, 0.90; η_f, 0.96; h, 18,900 Btu/lb; C_v, 0.97; ε, 1.00.)

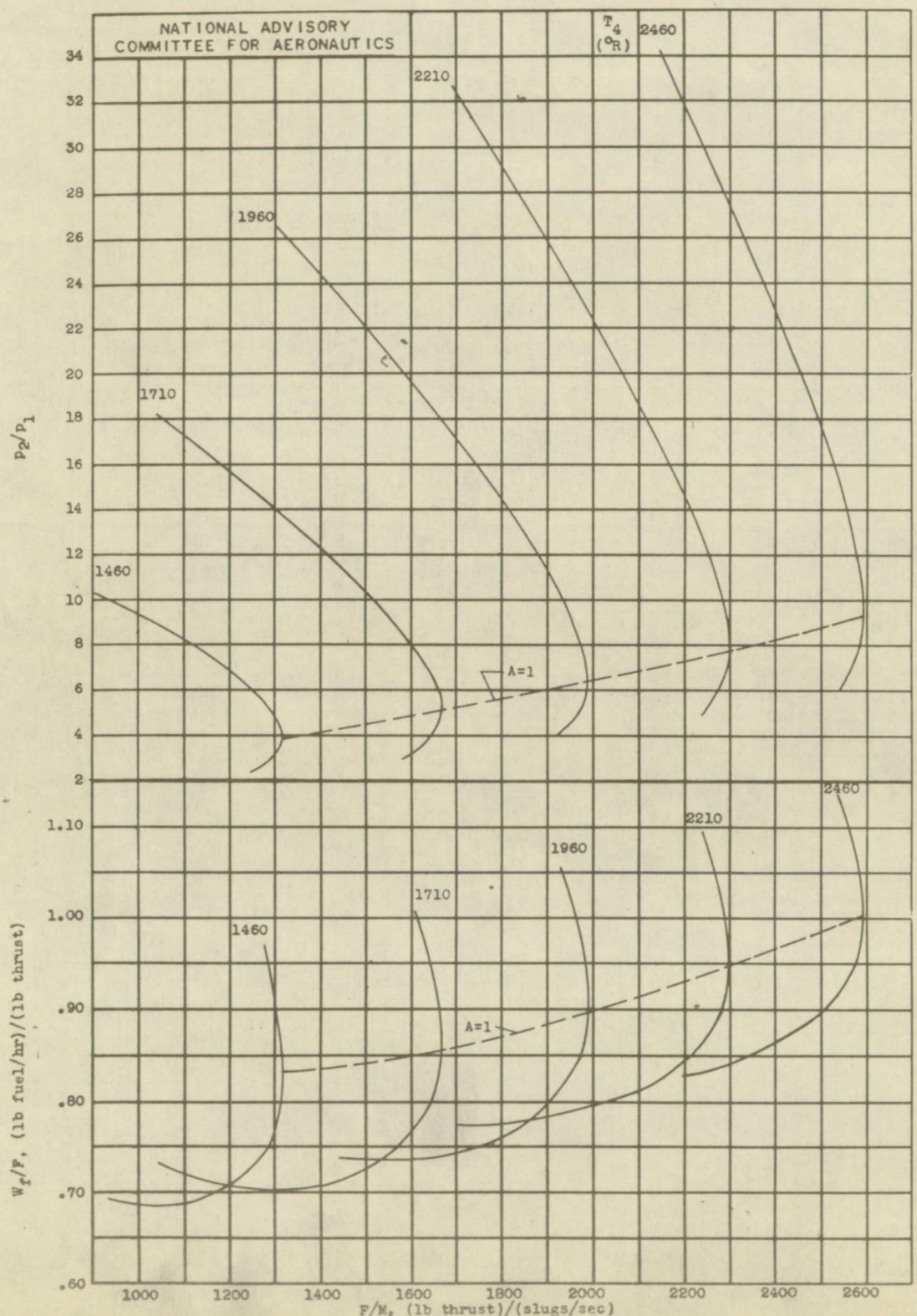

(a) V_o, 0 feet per second; T_o, 519° R.

Figure 9. - Compressor pressure ratio and fuel rate per unit thrust for various thrusts per unit mass rate of air flow and combustion-chamber discharge temperatures for illustrative case. (η_c, 0.85; η_t, 0.90; η_f, 0.96; h, 18,900 Btu/lb; C_v, 0.97; ϵ, 1.00.)

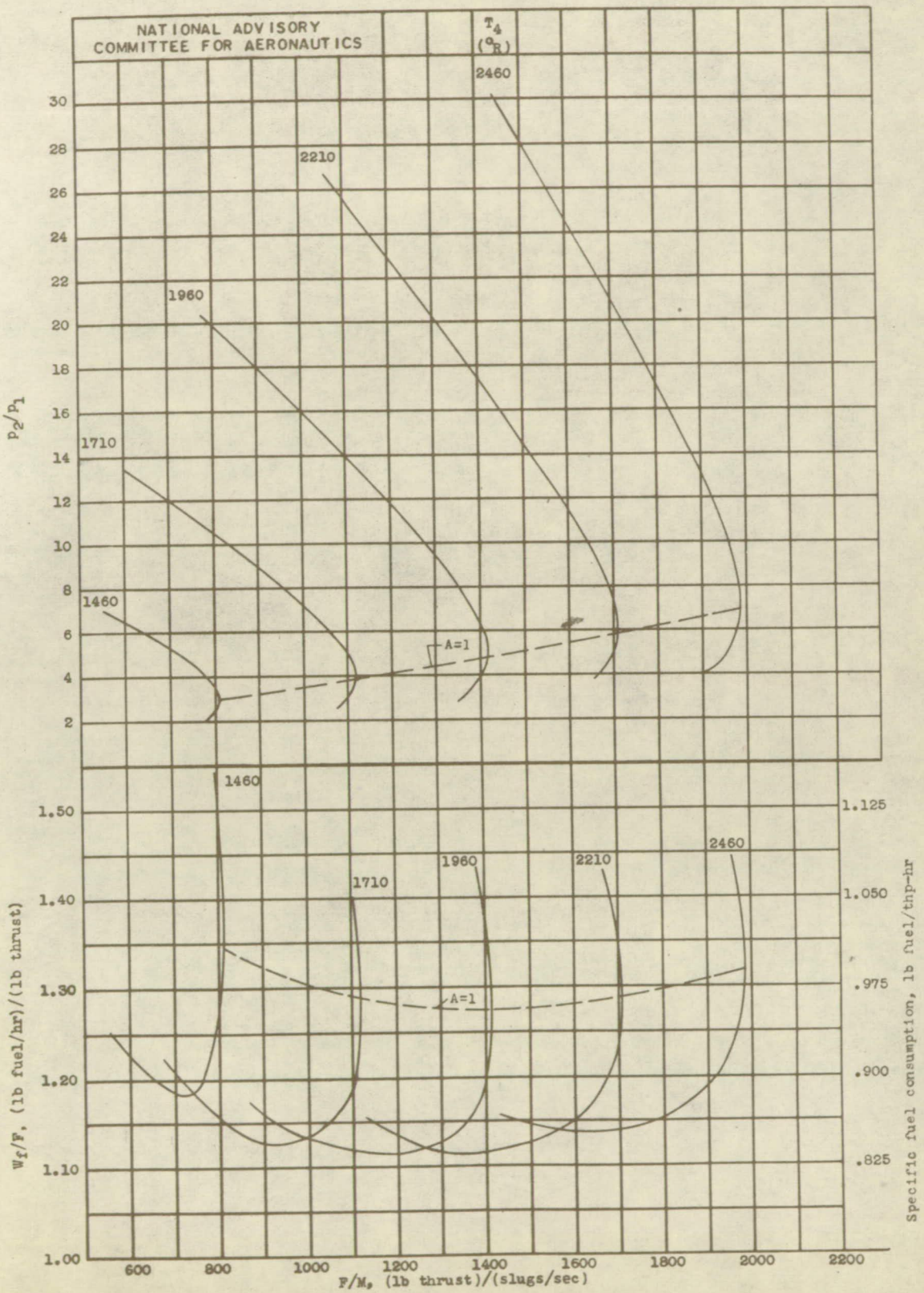

(b) V_o, 733 feet per second; T_o, 519° R.

Figure 9. - Continued.

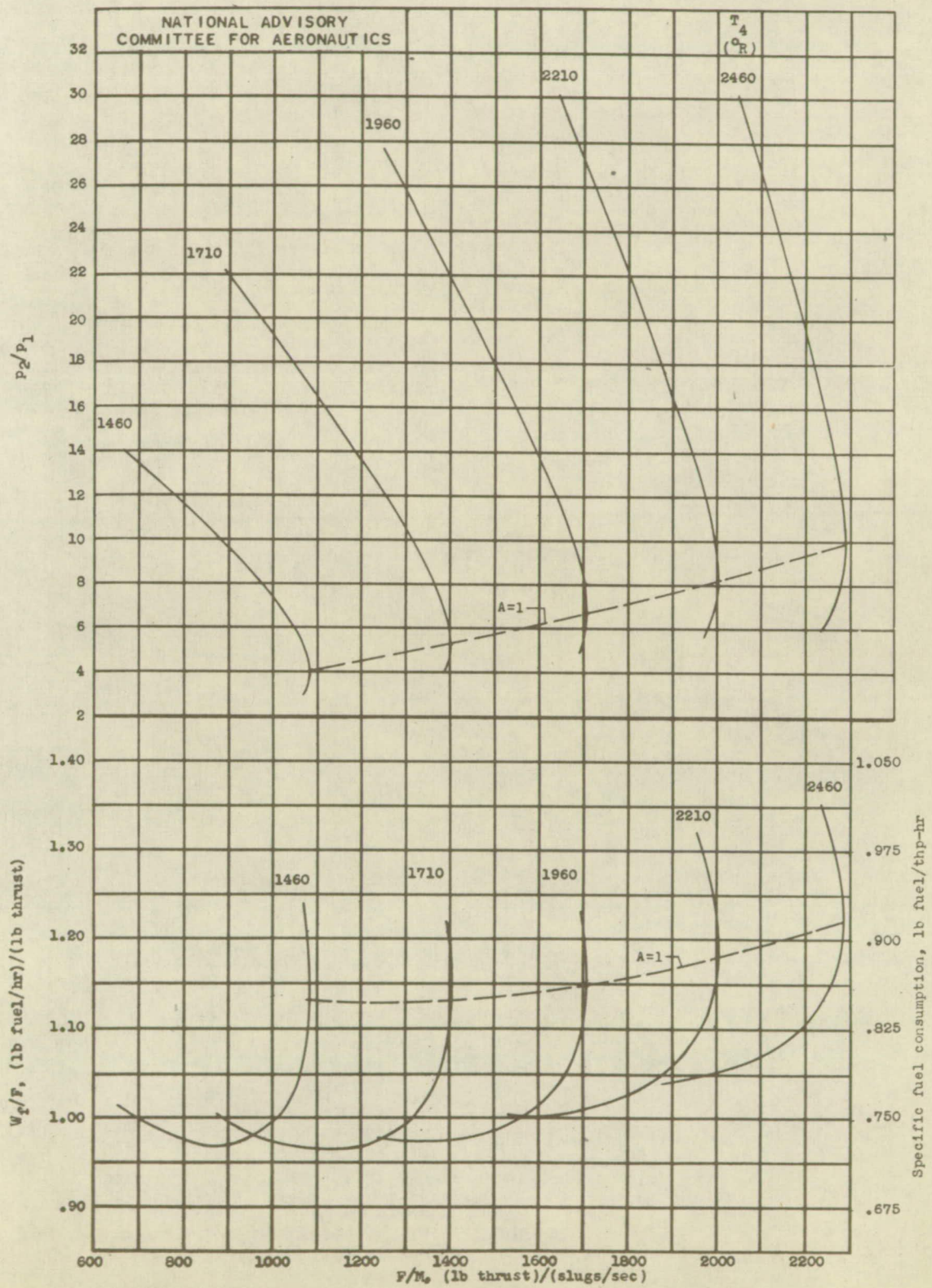

(c) V_0, 733 feet per second; T_0, 412° R.

Figure 9. - Concluded.

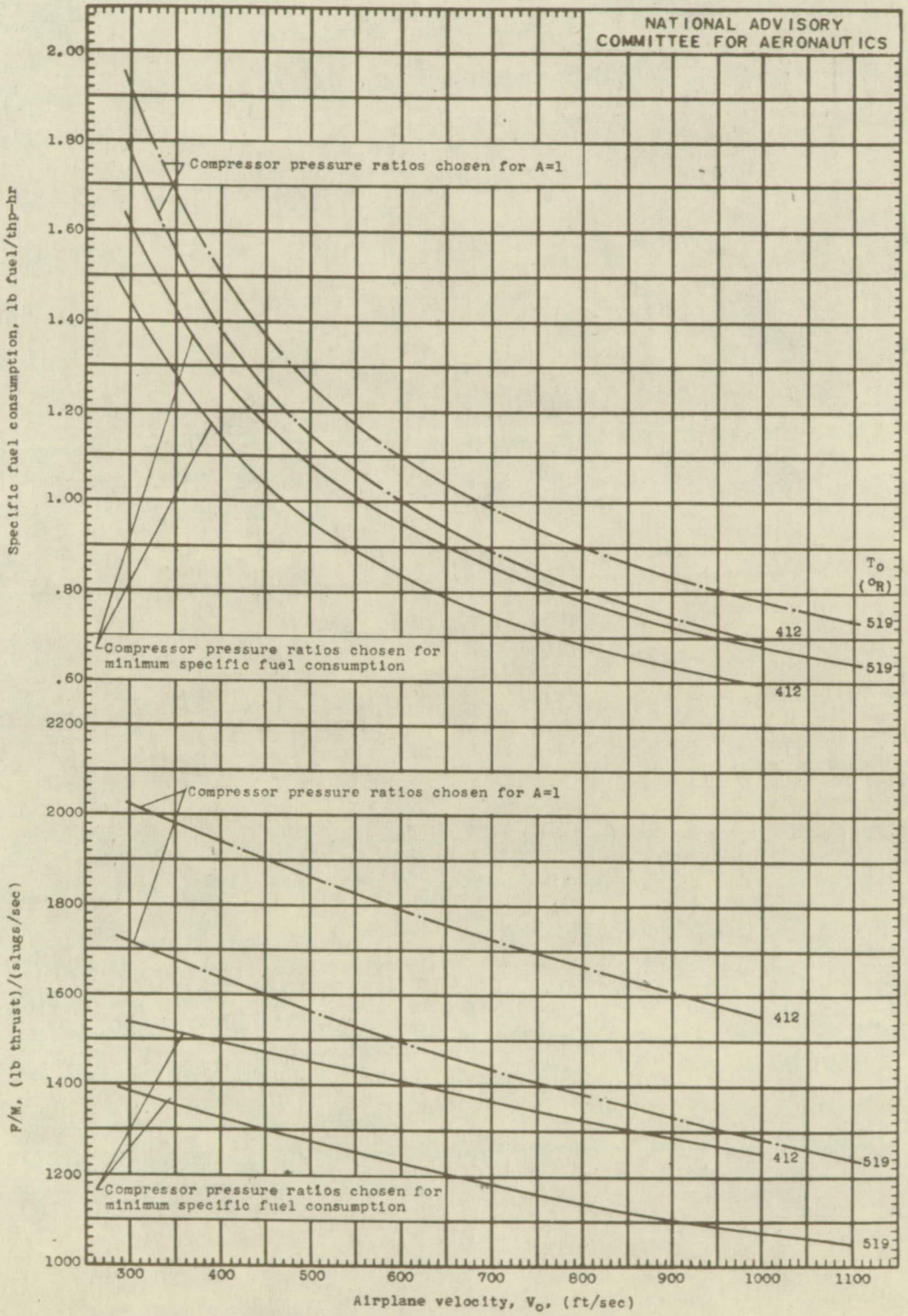

(a) Specific fuel consumption and thrust per unit air flow at various airplane velocities.

Figure 10.- Performance of jet-propulsion unit at conditions for minimum specific fuel consumption and for pressure ratios giving A=1 for illustrative case. (T_4, 1960° R: η_c, 0.85; η_t, 0.90; η_f, 0.96; C_v, 0.97; h, 18,900 Btu/lb; ϵ, 1.00.)

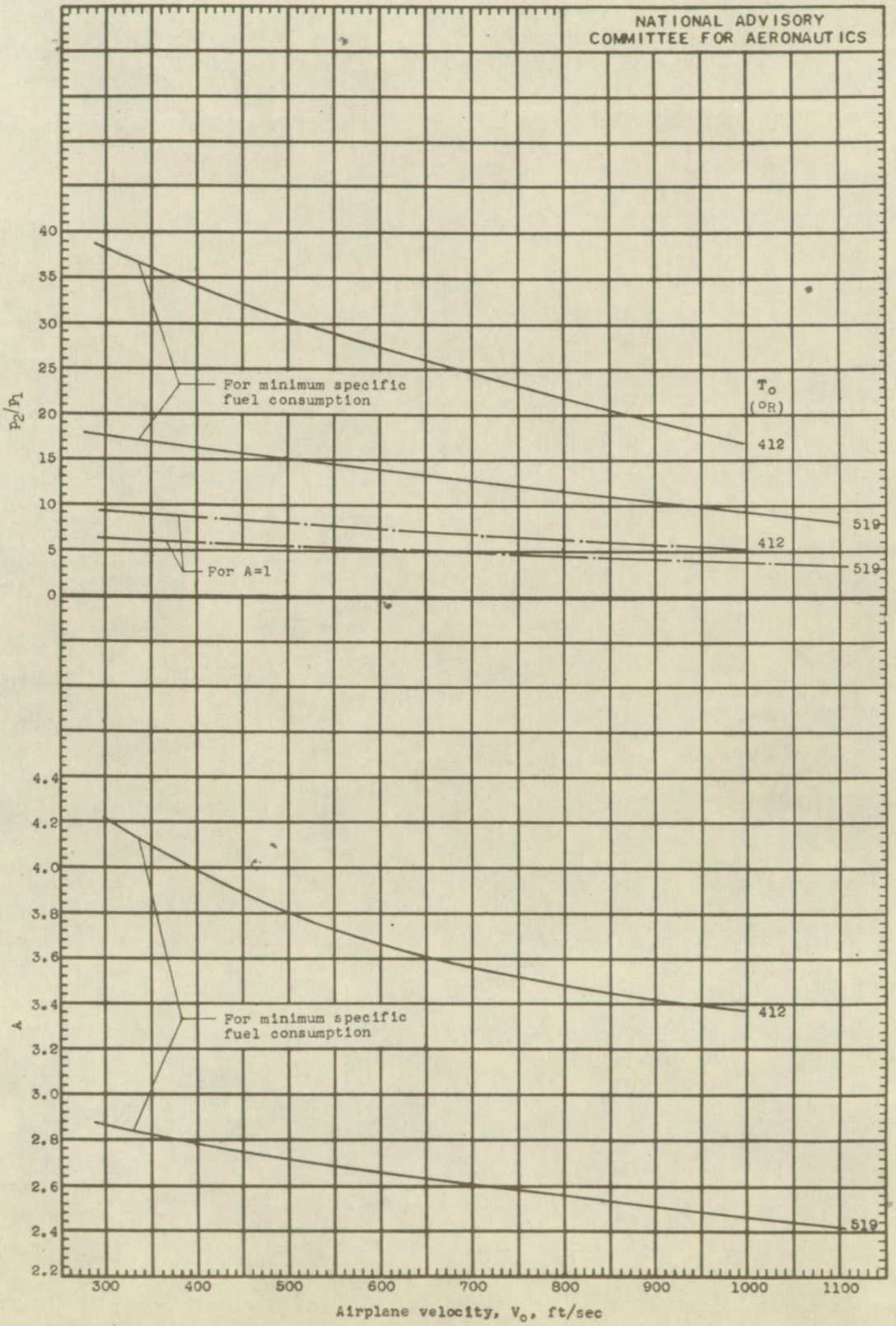

(b) Compressor pressure ratios and A at various airplane velocities.

Figure 10.- Concluded.

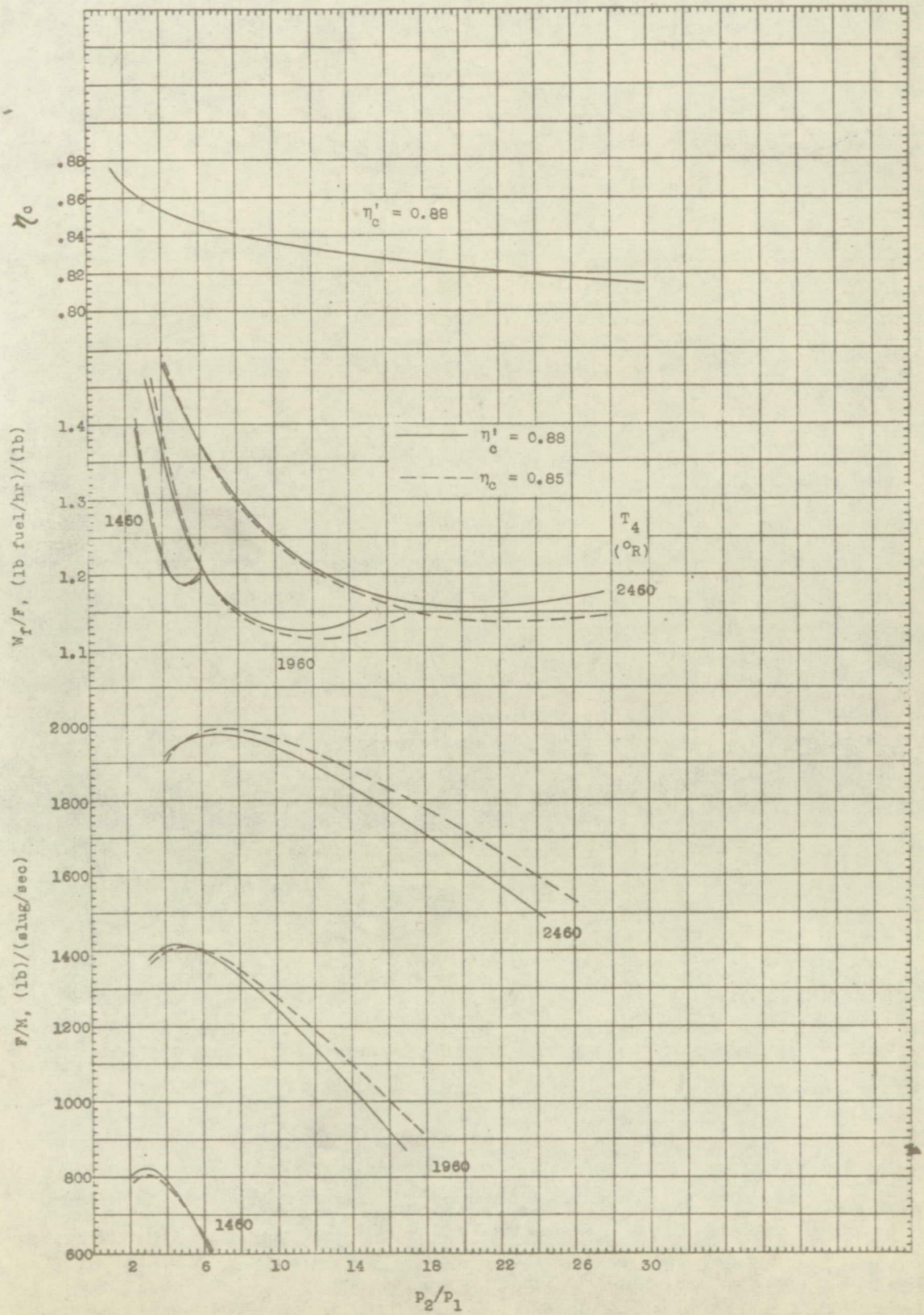

Figure 11. - Comparison of performance with constant η_c and with constant η_c' at various compressor pressure ratios. (V_o = 733 ft/ sec; T_o = 519° R; η_t = 0.90; η_f = 0.96; h = 18,900 Btu/lb; C_v = 0.97; ϵ = 1.00).

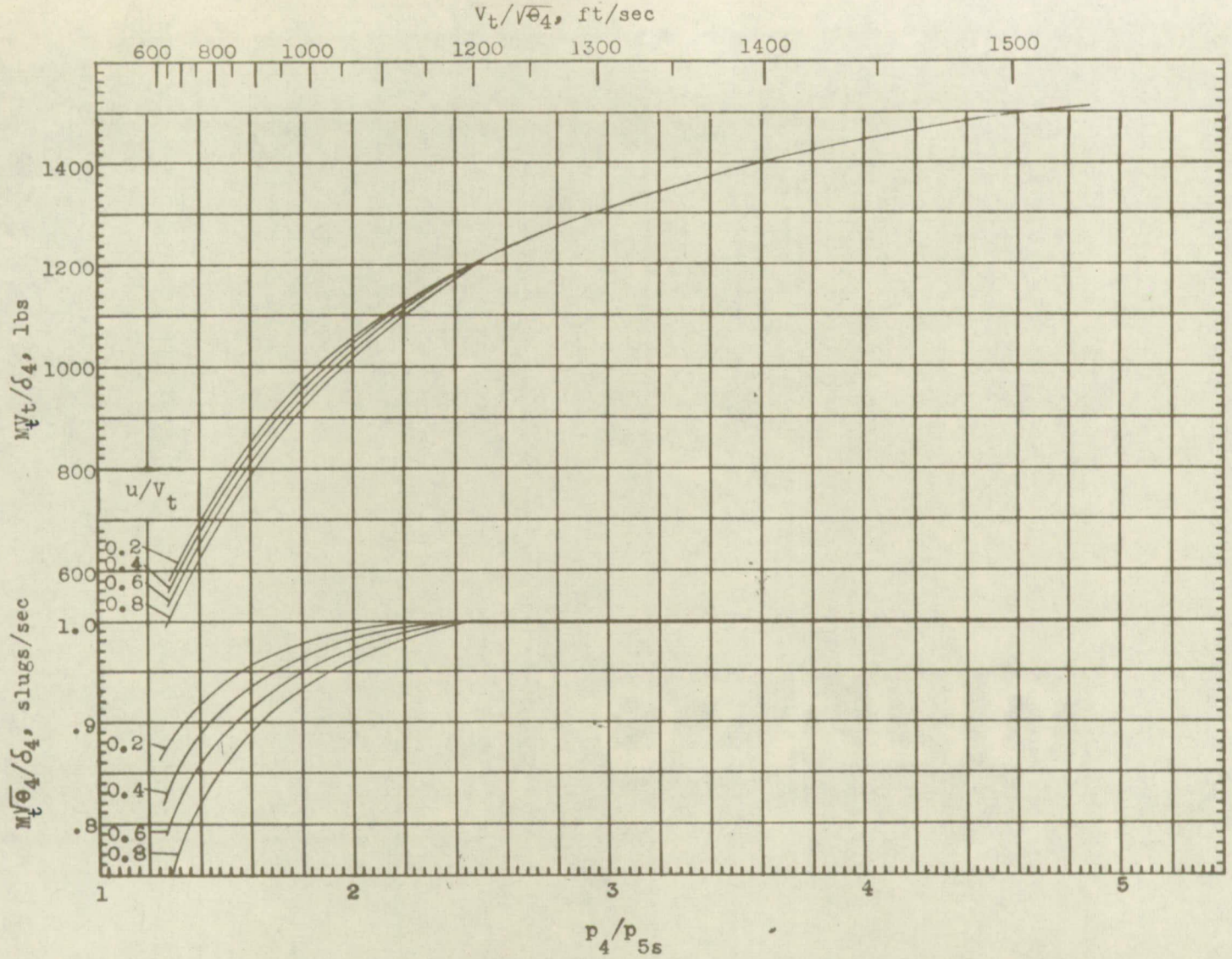

(a) Mass flow characteristics.

Figure 12. - Single stage turbine characteristics.

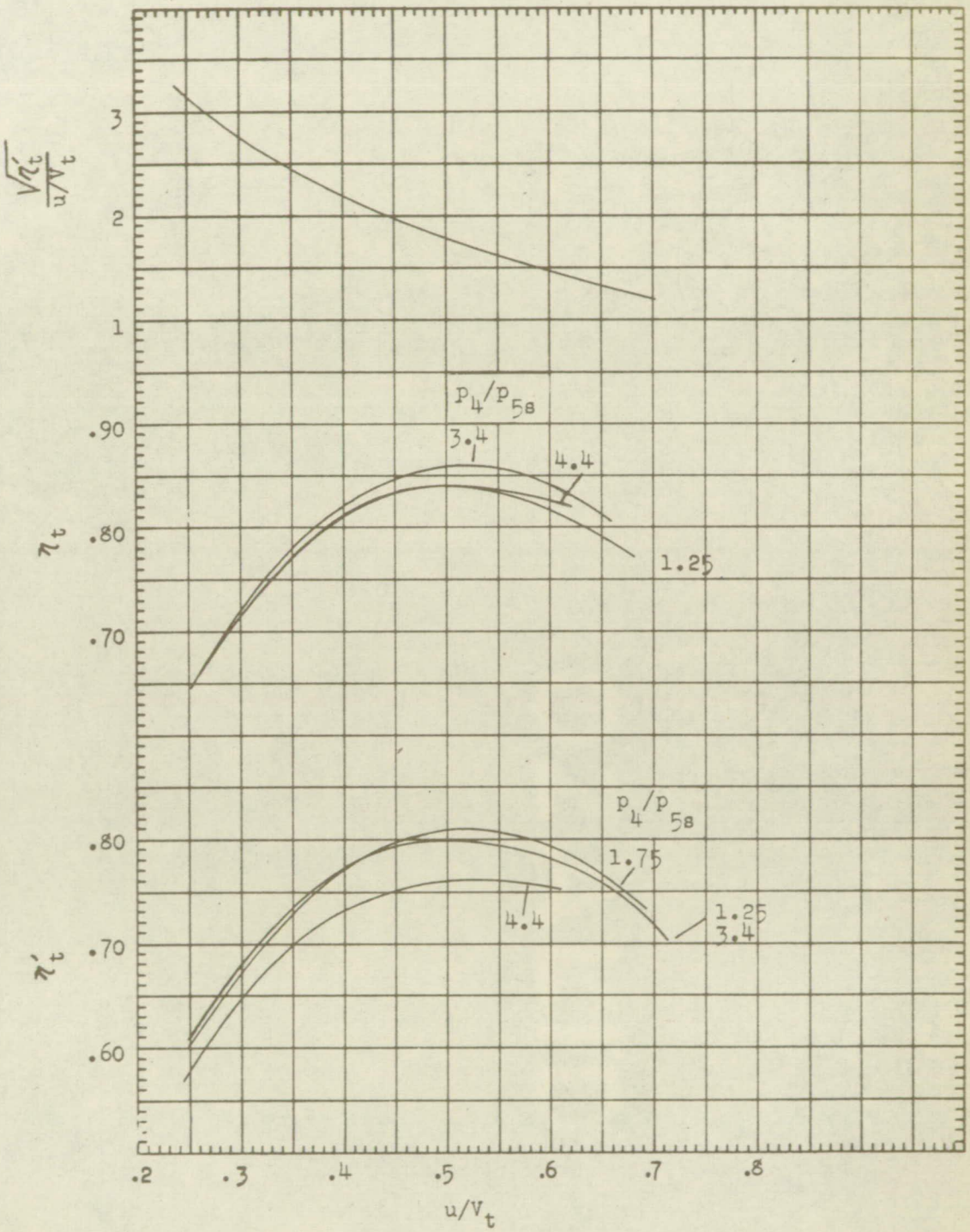

(b) Efficiency characteristics.

Figure 12. - Concluded. Characteristics of a single stage turbine.

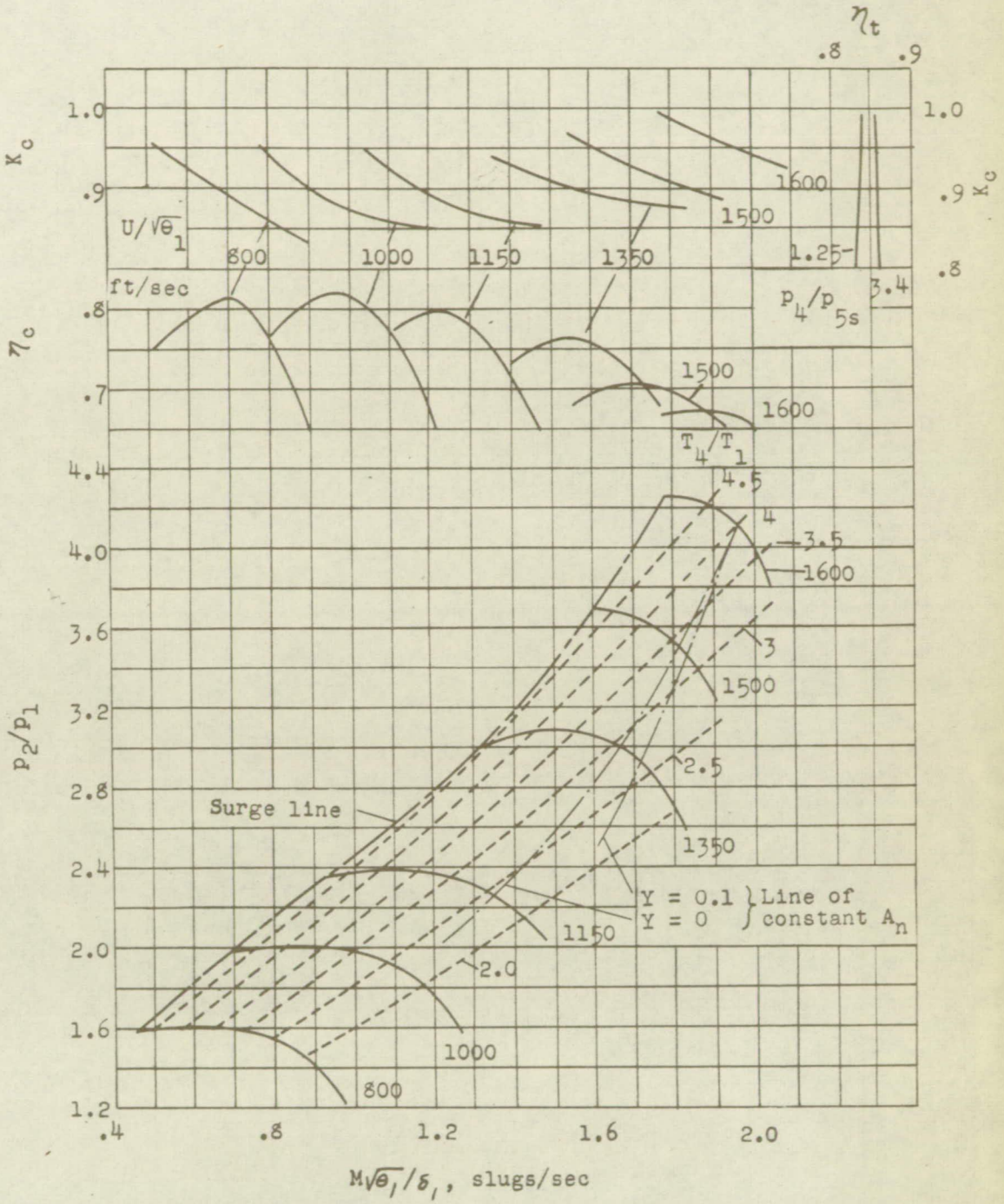

Figure 13. - Characteristics of a centrifugal compressor.

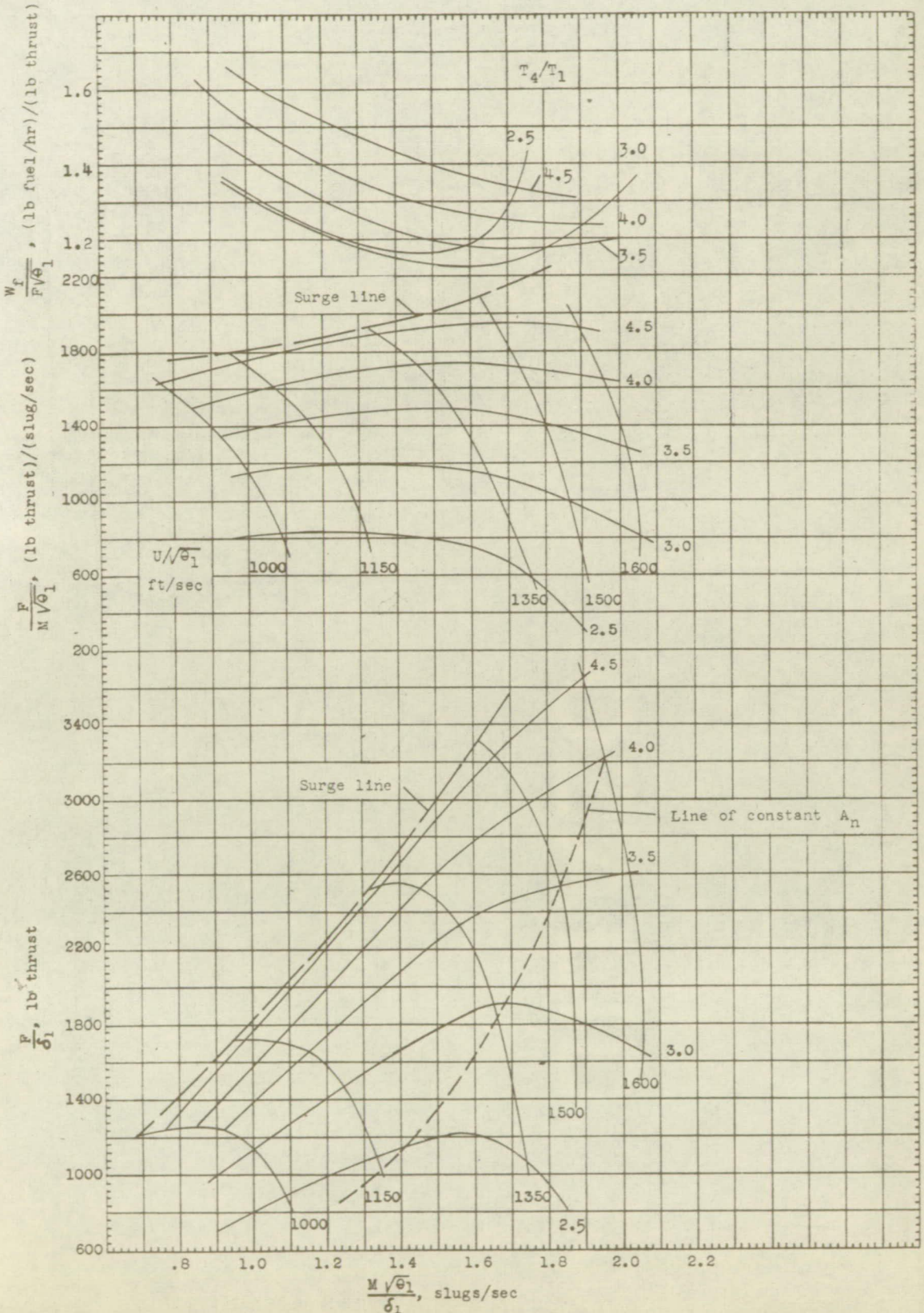

(a) Y = 0; flight Mach No. = 0.

Figure 14. - Performance of turbojet engine with centrifugal compressor. (η_f = 0.96; C_v = 0.97; ϵ = 1.00; h = 18,900 Btu/lb).

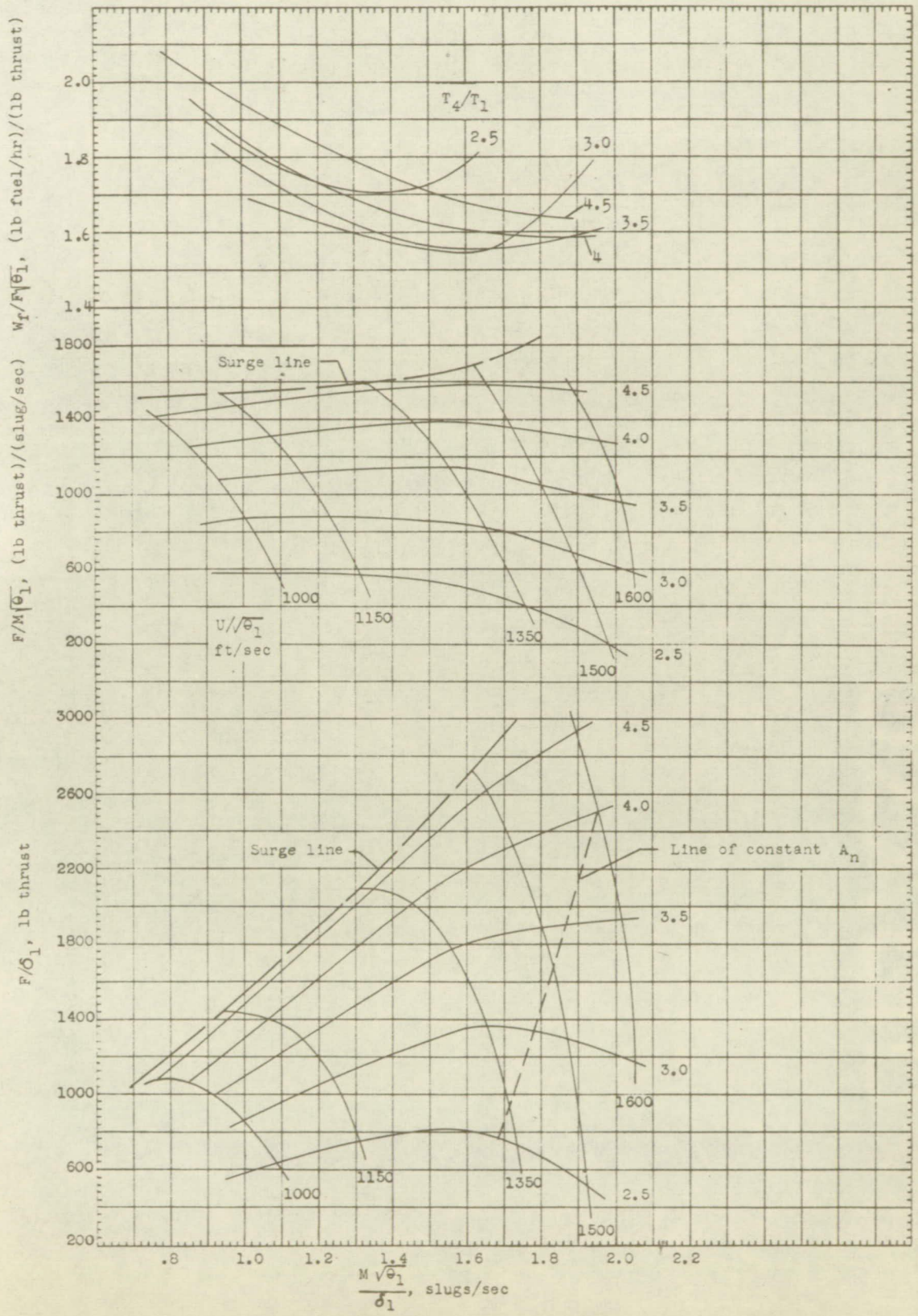

(b) Y = 0.1; flight Mach No. = 0.707.

Figure 14. - Concluded. Performance of turbojet engine with centrifugal compressor. (η_f = 0.96; C_v = 0.97; ϵ = 1.00; h = 18,900 Btu/lb).

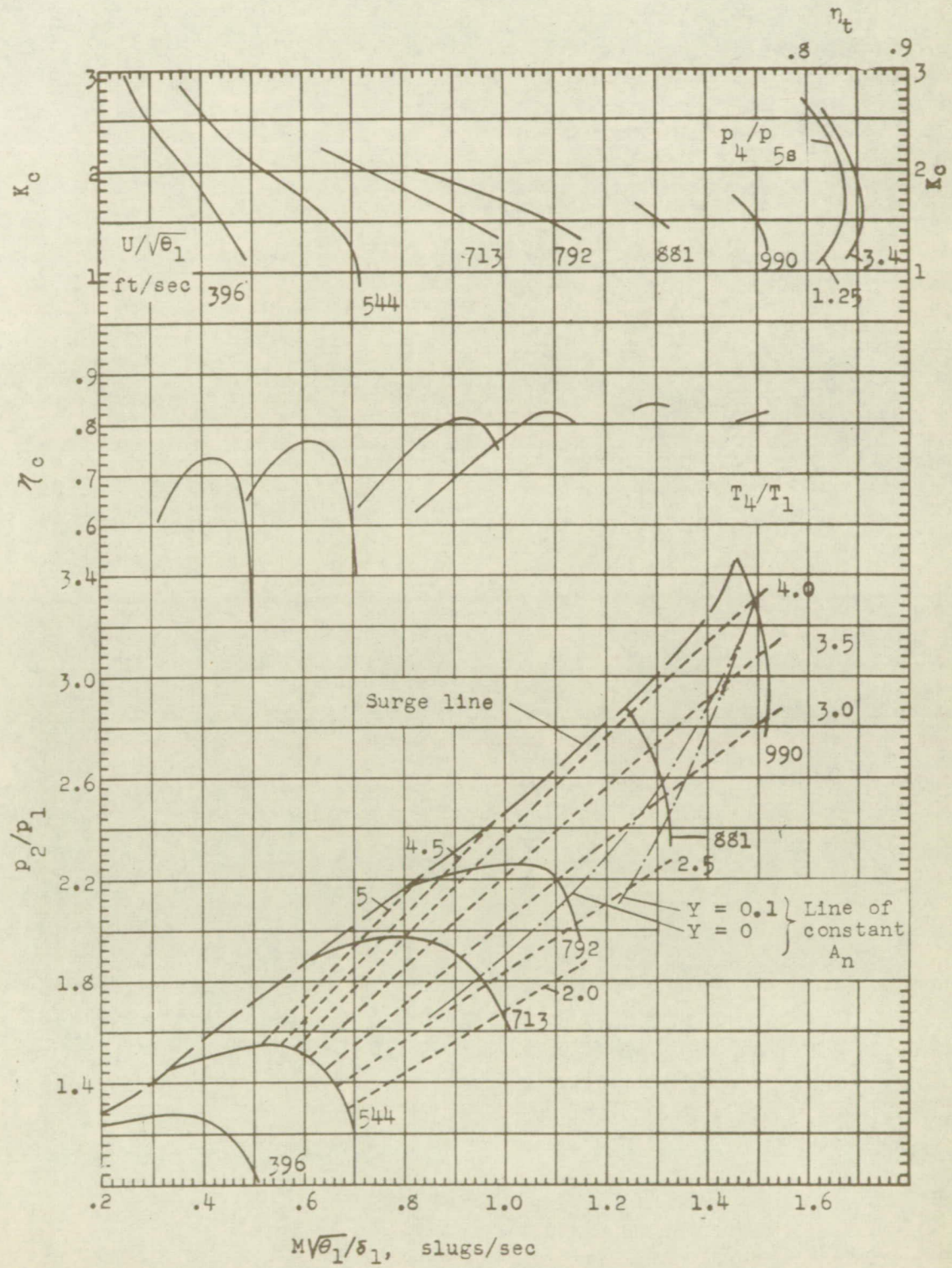

Figure 15. - Characteristics of an axial-flow compressor.

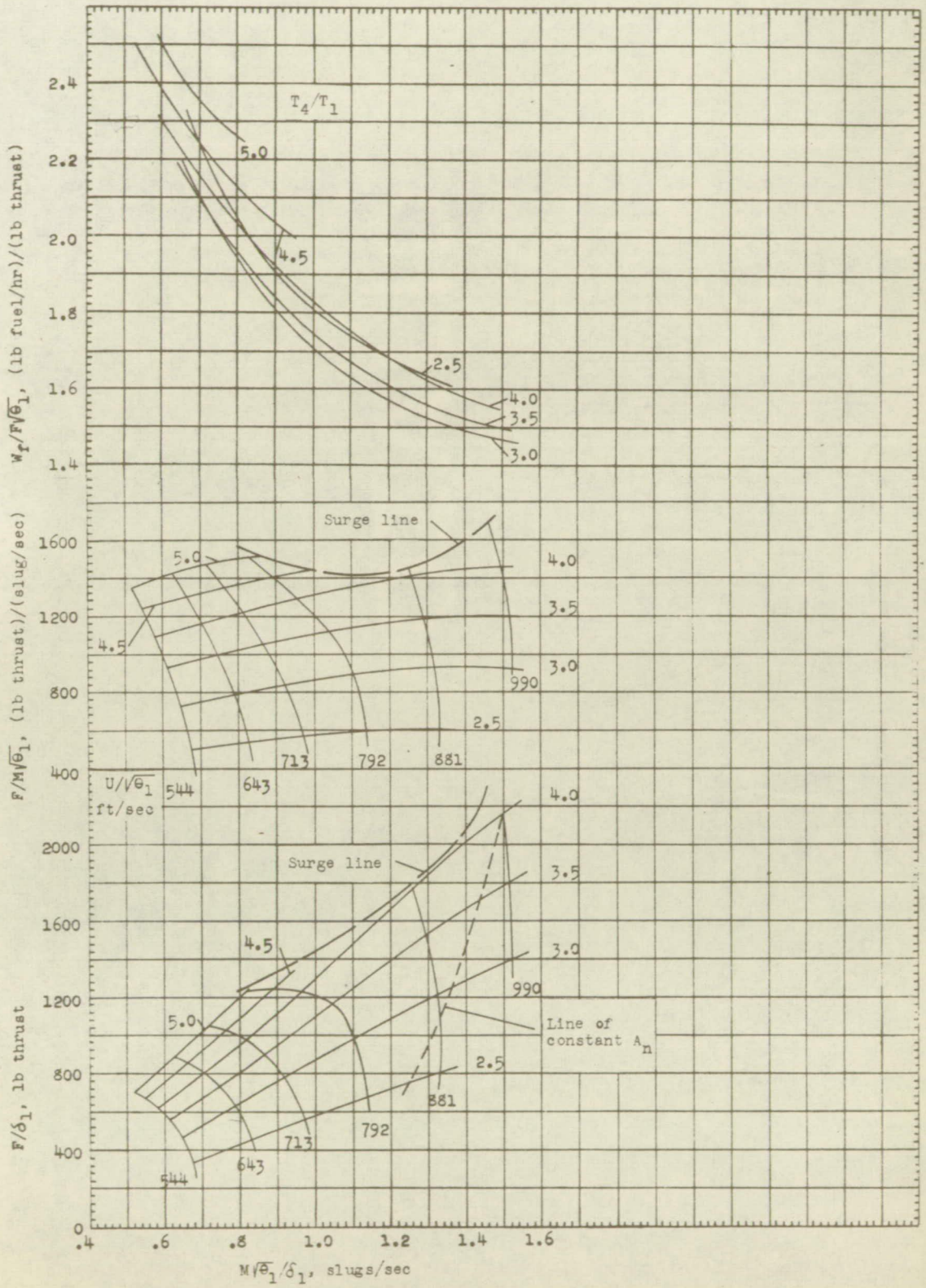

(b) Y = 0.1, flight Mach number = 0.707.

Figure 16. - Concluded. Performance of turbojet engine with axial compressor (η_f = 0.96; C_v = 0.97; ϵ = 1.00; h = 18,900 Btu/lb).

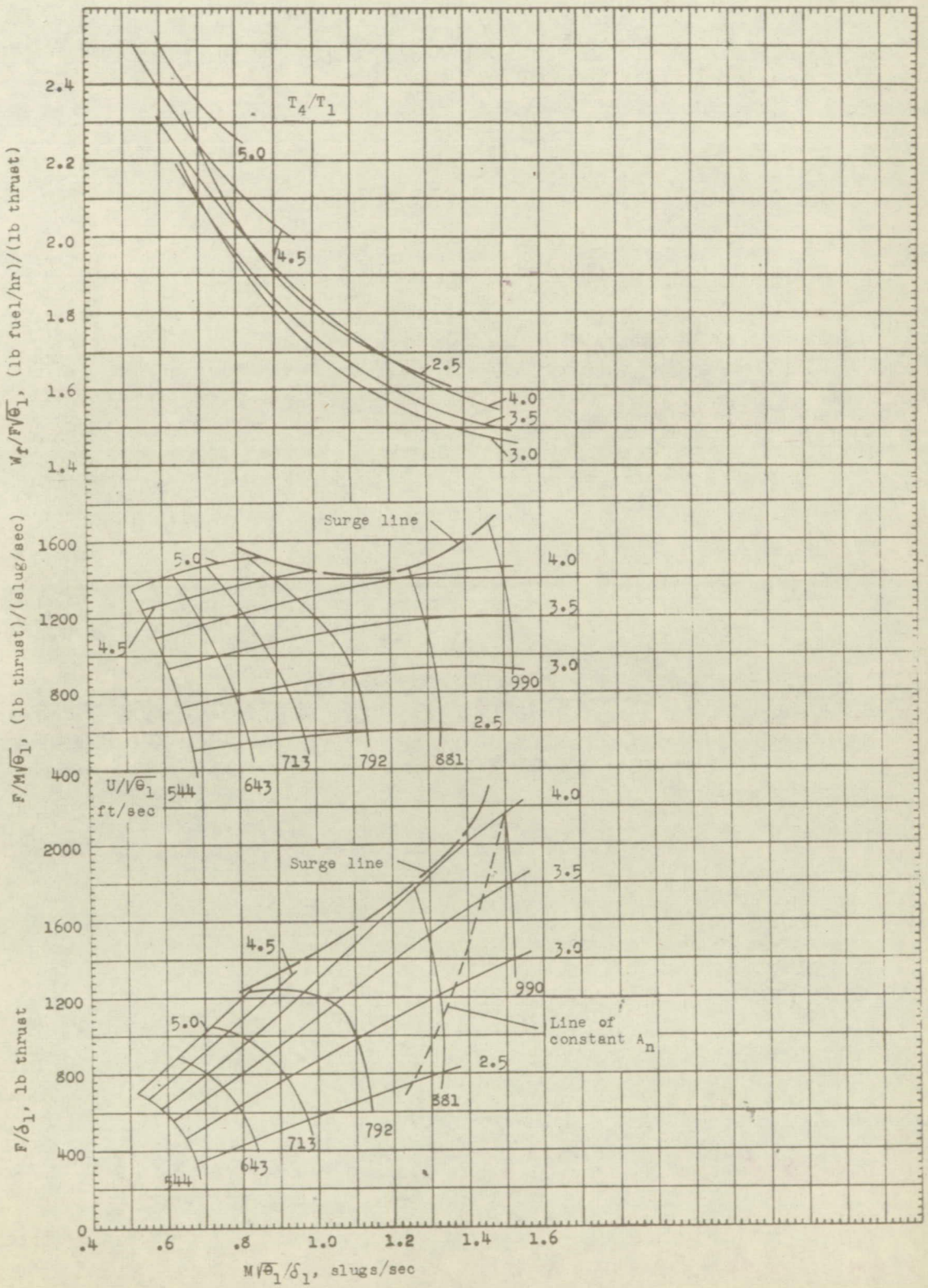

(b) Y = 0.1, flight Mach number = 0.707.

Figure 16. - Concluded. Performance of turbojet engine with axial compressor (η_f = 0.96; C_v = 0.97; ϵ = 1.00; h = 18,900 Btu/lb).